HUMMR, a hypoxia- and HIF-1α–inducible protein, alters mitochondrial distribution and transport

Yan Li,[1,3] Seung Lim,[5] David Hoffman,[4] Pontus Aspenstrom,[6] Howard J. Federoff,[5] and David A. Rempe[1,2,3]

[1]Department of Neurology, Center for Neural Development and Disease, [2]Interdepartmental Graduate Program in Neuroscience, [3]Interdepartmental Graduate Program in Biomedical Genetics, and [4]Department of Anesthesiology, University of Rochester School of Medicine & Dentistry, Rochester, NY 14642
[5]Georgetown University Medical Center, Washington, DC 20057
[6]Department of Microbiology, Tumour and Cell Biology, Karolinska Institute, SE-171 77 Stockholm, Sweden

Mitochondrial transport is critical for maintenance of normal neuronal function. Here, we identify a novel mitochondria protein, hypoxia up-regulated mitochondrial movement regulator (HUMMR), which is expressed in neurons and is markedly induced by hypoxia-inducible factor 1 α (HIF-1α). Interestingly, HUMMR interacts with Miro-1 and Miro-2, mitochondrial proteins that are critical for mediating mitochondrial transport. Interestingly, knockdown of HUMMR or HIF-1 function in neurons exposed to hypoxia markedly reduces mitochondrial content in axons. Because mitochondrial transport and distribution are inextricably linked, the impact of reduced HUMMR function on the direction of mitochondrial transport was also explored. Loss of HUMMR function in hypoxia diminished the percentage of motile mitochondria moving in the anterograde direction and enhanced the percentage moving in the retrograde direction. Thus, HUMMR, a novel mitochondrial protein induced by HIF-1 and hypoxia, biases mitochondria transport in the anterograde direction. These findings have broad implications for maintenance of neuronal viability and function during physiological and pathological states.

Introduction

Hypoxia is a potentially injurious stimulus that evokes molecular responses to enhance oxygen delivery and maintain energy supply. Hypoxia-inducible factor 1 α (HIF-1α), a master regulator of the cellular response to hypoxia, is a transcription factor stabilized and activated during hypoxia (for reviews see Semenza, 2000a,b; Wenger, 2000; Kietzmann et al., 2001). Recent data supports an important role for HIF-1 in modulating mitochondrial function (Kim et al., 2006; Papandreou et al., 2006; Fukuda et al., 2007; Zhang et al., 2007). Two studies describe HIF-1–dependent induction of pyruvate dehydrogenase kinase-1, which reduces mitochondrial oxygen consumption and reactive oxygen species production during hypoxia (Kim et al., 2006; Papandreou et al., 2006). In addition, HIF-1 also alters electron transport chain function by mediating switching of a subunit of complex IV, allowing the mitochondria to fine tune electron transport function during hypoxia (Fukuda et al., 2007). Finally, HIF-1 activity suppresses mitochondrial DNA proliferation by suppression of c-Myc activity (Zhang et al., 2007), and enhances mitochondrial autophagy by inducing the expression of bNip-3 (Semenza, 2008; Zhang et al., 2008).

In highly polarized cell types, such as neurons, transport of mitochondria is essential for maintenance of neuronal health and is maintained through the actions of multiple anterograde and retrograde protein motors and adapters (Hollenbeck and Saxton, 2005; Verstreken et al., 2005; Chang and Reynolds, 2006; Ly and Verstreken, 2006; Frederick and Shaw, 2007). A protein conserved from yeast to mammals, Miro, is anchored in the outer mitochondrial membrane (OMM), and is necessary for mitochondrial transport (Fransson et al., 2003, 2006; Guo et al., 2005). *Drosophila* with loss of dMiro function display abnormal perinuclear clustering of mitochondria (Guo et al., 2005), as do yeast lacking Gem 1P (Miro orthologue; Frederick et al., 2004). In addition, loss of dMiro function restricts mitochondrial transport and

Correspondence to David A. Rempe:david_rempe@urmc.rochester.edu

Abbreviations used in this paper: DIV, day in vitro; GRIF-1, $GABA_A$ receptor-interacting factor 1; HIF-1α, hypoxia-inducible factor 1 α; HUMMR, hypoxia up-regulated mitochondrial movement regulator; ICC, immunocytochemistry; IMM, inner mitochondrial membrane; IMS, intermembrane space; IP, immunoprecipitation; MLS, mitochondrial localization signal; OMM, outer mitochondrial membrane; scrRNA, scrambled RNA; shRNA, small hairpin RNA; TMD, transmembrane domain.

The Rockefeller University Press $30.00
J. Cell Biol. Vol. 185 No. 6 1065–1081
www.jcb.org/cgi/doi/10.1083/jcb.200811033

impairs synaptic function during trains of stimulation at the neuromuscular junction in *Drosophila* (Guo et al., 2005). Milton binds to the dMiro and tethers the mitochondria to the kinesin heavy chain. The mammalian orthologues of Milton are $GABA_A$ receptor-interacting factor 1 (GRIF-1) and O-linked *N*-acetylglucosamine transferase-interacting protein (OIP106). Similar to dMiro, *Drosophila* with loss of Milton function have restricted mitochondrial transport and synaptic dysfunction (Gorska-Andrzejak et al., 2003; Glater et al., 2006). Recent studies suggests that Miro function and calcium-dependent control of mitochondrial transport is important for distributing mitochondria to the synapses and altering neuronal death (Macaskill et al., 2009b; Wang and Schwarz, 2009). Therefore, Miro, Milton, and the kinesins are integral to maintenance of mitochondrial transport influencing synaptic function and neuronal health.

In this paper, we describe a mitochondrial protein involved in mitochondrial transport, which we rename hypoxia up-regulated mitochondrial movement regulator (HUMMR). In astrocytes, neurons, and whole brain, HUMMR abundance is low in normoxia, but it is markedly induced by hypoxia through a HIF-1–dependent process. A prior study named this protein corneal endothelium-specific protein-1 (Kinouchi et al., 2006), but did not describe its function. HUMMR specifically localizes to mitochondria and interacts with the Miros. Loss of HUMMR or HIF-1 function significantly reduces the number of mitochondria in the axon in neurons exposed to hypoxia. Interestingly, loss of HUMMR or HIF-1 function diminishes the percentage of motile mitochondria moving in the anterograde direction, but increases the percentage moving in the retrograde direction. Because HIF-1 is induced during hypoxia, ischemia, and Alzheimer's disease, these results have broad implications for mitochondrial transport and its resultant effects on synaptic and neuronal function during disease.

Results

HIF-1α induces a unique mitochondrial protein, HUMMR

Microarray technology (CodeLink) was used to search for HIF-1–dependent targets. Conditional loss of HIF-1α function was achieved in neuronal cultures using bigenic mice with a floxed HIF-1α gene locus ($HIF\text{-}1\alpha^{F/F}$; Ryan et al., 2000) and cre recombinase expression (synapsin I cre; Zhu et al., 2001). Known HIF-1 targets (see Table S1) and a transcript of unknown function (available from GenBank/EMBL/DDBJ under accession no. NM_026358) were identified as HIF-1 targets. The transcript has the same sequence as corneal endothelium-specific protein (Kinouchi et al., 2006). We elected to rename this protein HUMMR to better reflect its regulation and function.

Quantitative PCR confirmed the hypoxic induction of HUMMR transcript and its dependence on HIF-1 function (Fig. 1). Similar to our prior reports (Rempe et al., 2007; Vangeison et al., 2008), loss of HIF-1 function was induced in astrocytes or neurons in vitro, and in brain cortex in vivo using $HIF\text{-}1\alpha^{F/F}$ mice (Ryan et al., 2000) crossed with different cre recombinase–expressing mice (Fig. 1 A). Loss of HIF-1 function inhibited hypoxia-induced HUMMR transcript expression (Fig. 1 B). Several (16) putative hypoxic response elements (5′-RCGTG-3′) were contained within the 5′ promoter, introns, and 3′ untranslated region of HUMMR, which suggests that HUMMR is a HIF-1 target (Fig. 1 G).

To examine HUMMR protein regulation, an anti–mouse HUMMR polyclonal antibody was produced. In agreement with a prior study (Kinouchi et al., 2006), the molecular weight of HUMMR was near 50 kD (Fig. 1 C), and was expressed in brain, testes, and ovary (Fig. 1 F). HUMMR protein abundance was markedly induced by hypoxia in neurons and astrocytes, which was prevented by loss of HIF-1α function (Fig. 1, D and E). Analysis of the amino-acid sequence of HUMMR predicted a mitochondrial localization signal (MLS) at the amino terminus (MitoProtII; Claros and Vincens, 1996) and a transmembrane domain (TMD) following the MLS (Fig. 2 A; Tusnady and Simon, 2001). As reported previously in corneal cells (Kinouchi et al., 2006), immunocytochemistry (ICC) confirmed the mitochondrial localization of HUMMR (Fig. 2 B).

HUMMR induces collapse of the mitochondrial network, which is not reversed by inhibiting mitochondrial fusion or enhancing mitochondrial fission

Transfection of a C-terminal Flag-tagged version of HUMMR (HUMMR-Flag) collapsed the mitochondrial network around the nucleus in 80% of astrocytes (Fig. 3, B and C), which was not observed with mito-YFP (Fig. 3 A; Llopis et al., 1998). HUMMR-Flag did not colocalize with protein disulfide isomerase or GM130 (Fig. 3, D and E), which label the ER and the Golgi apparatus, respectively. The actin and microtubule intracellular cytoskeleton structure was not altered by HUMMR-Flag (Fig. S1).

To determine if HUMMR may increase mitochondrial fusion, which can induce a similar perinuclear clumping of mitochondria (Santel et al., 2003), we transfected HUMMR-Flag into immortalized mouse embryonic fibroblasts with knockout of both mitofusin 1 and 2 function (Chen et al., 2003). Loss of mitofusin 1 and mitofusin 2 function did not prevent HUMMR-induced mitochondria network collapse (Fig. S2 A). Similarly, we examined the impact of expressing mitochondrial fission proteins on HUMMR-induced mitochondrial network collapse. Although many cells transfected with human Fis (hFis) displayed fragmented mitochondria, neither Dlp1 nor hFis inhibited HUMMR-induced mitochondrial network collapse (Fig. S2, B–E).

HUMMR forms a protein complex with Miro-1, Miro-2, OIP106, and GRIF-1, but not h-Fis

Because transfection of Milton or constitutively active Miro collapses the mitochondrial network (Stowers et al., 2002; Fransson et al., 2003; Glater et al., 2006), we examined potential interactions between HUMMR and these proteins, which are critical for mitochondria transport. Immunoprecipitations (IPs) were performed after cotransfection of Myc-tagged Miro-1 or Miro-2 (Myc–Miro-1 and Myc–Miro-2) with V5-tagged HUMMR (HUMMR-V5). Compared with the endogenous form, transfected Miro-2 was 8.5-fold more abundant. Direct comparisons of transfected and endogenous HUMMR abundance could not be performed because transfected HUMMR was derived from mice, and endogenous HUMMR in HEK-293 cells is of

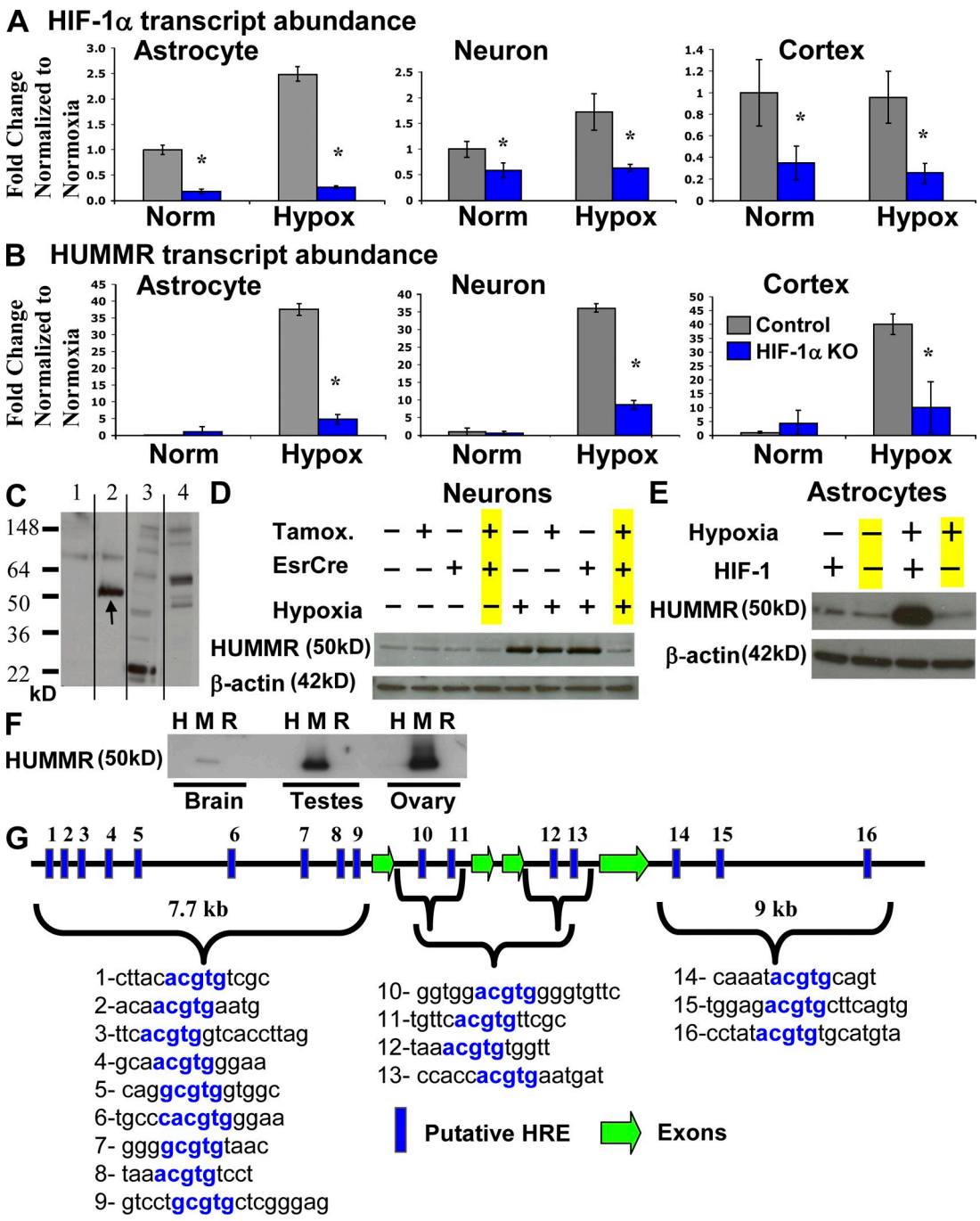

Figure 1. **Hypoxia induces transcriptional and translational up-regulation of HUMMR.** (A) HIF-1α exon 2 transcript abundance was reduced in astrocyte cultures, neuronal cultures, and brain cortex. In each case, HIF-1$^{F/F}$ was the genotype of controls, whereas the cultures with loss of HIF-1α function were derived from HIF-1$^{F/F}$::hGFAPcre (astrocytes in A, B, and E), HIF-1$^{F/F}$::SynCre (neurons in A and B), HIF-1$^{F/F}$::EsrCre (neurons in D), or HIF-1$^{F/F}$::hGFAPcre (cortex in A and B) mice. (B) Loss of HIF-1α function largely eliminated the hypoxia-mediated induction of HUMMR transcript. The transcript abundance in A and B was normalized to its level in normoxia. (C) Unlike the preimmune serums (lanes 3 and 4), a specific protein band was identified near 50 kD by the HUMMR rabbit polyclonal antibody (arrow in lane 2), which was eliminated by preincubation of the membrane with HUMMR blocking peptide (lane 1). Black lines indicate that intervening lanes have been spliced out. (D and E) Hypoxia induced HUMMR protein abundance in primary neuron (D) and astrocyte (E) cultures, which was largely eliminated by loss of HIF-1 function (highlighted in yellow). EsrCre, tamoxifen-regulated Cre recombinase; Tamox., Tamoxifen. (F) Using IB, HUMMR was identified in brain, testes, and ovary from mouse. H, human; M, mouse; R, rat. (G) A schematic diagram demonstrating multiple putative hypoxic response elements (HREs; blue boxes; containing 5′-RCGTG-3′ core) in the promoter and introns of the genomic sequence of HUMMR. The specific DNA sequences of the putative HREs are detailed below the diagram.

human origin. IPs using V5 or Myc antibodies demonstrate that HUMMR coprecipitates with the Miros, which was not observed in controls (Fig. 4, A–C). No interaction was identified between HUMMR and hFis, which like Miro is anchored in the OMM (Fig. 4 D). Finally, an Xpress-tagged version of OIP106 and Flag-tagged version of GRIF-1 coprecipitated with HUMMR-V5 (Fig. 4, E–F), as would be expected for a protein interacting with Miro.

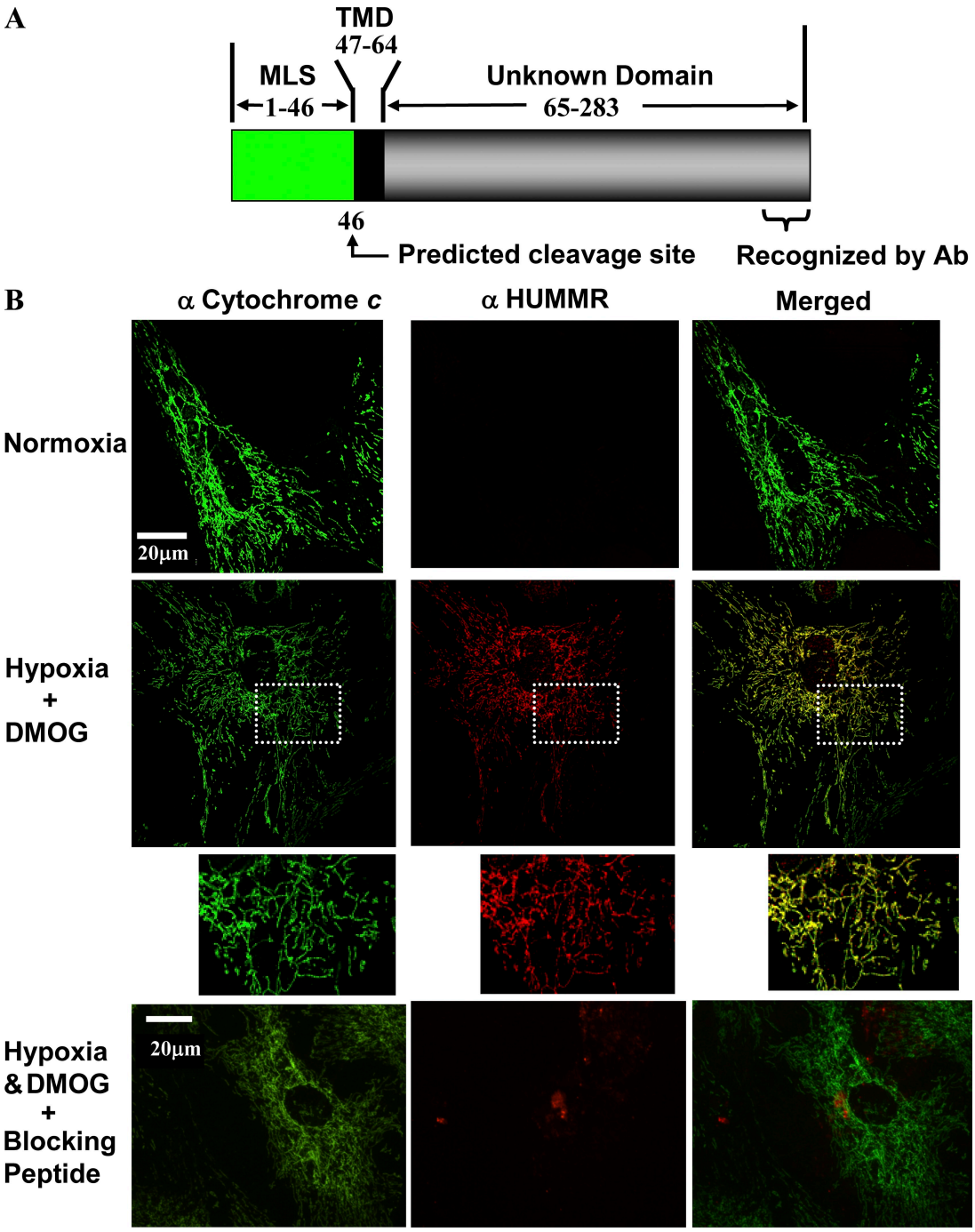

Figure 2. **Hypoxia-induced HUMMR is localized to mitochondria.** (A) A schematic diagram of HUMMR with MLS, TMD, the predicted cleavage site, a domain of unknown function, and the area of protein recognized by the antibody. Numbers indicate amino acids. (B) A combination of hypoxia- and dimethyloxaloylglycine-induced expression of HUMMR in astrocyte mitochondria (identified by cytochrome *c*). A blocking peptide of HUMMR eliminated the mitochondrial labeling. All data were replicated in triplicate in three independent experiments. The boxed regions show the areas enlarged below.

The interactions of endogenous Miro and HUMMR were examined using rabbit polyclonal antibodies that recognize human Miro-2 or human HUMMR. The Miro-2 antibody identified a band near 70 kD, which was lost when isolated mitochondria were exposed to trypsin, confirming its location in the OMM (Fig. S3). The HUMMR antibody identified a unique 40-kD band, which had an expression pattern similar to that of mouse HUMMR (Fig. 1), in agreement with a prior study (Kinouchi et al., 2006). Using these antibodies, endogenous human HUMMR (hHUMMR) coprecipitated with Miro-2 from protein lysates obtained from HEK-293 cells (Fig. 4, G and H).

HUMMR alters the localization of GRIF-1 and colocalizes with Miro-1, Miro-2, OIP106, and GRIF-1

Given that HUMMR forms a protein complex with Miro-1, Miro-2, GRIF-1, and OIP106, we examined if these proteins colocalize with HUMMR. As determined by ICC, Myc–Miro-1 and

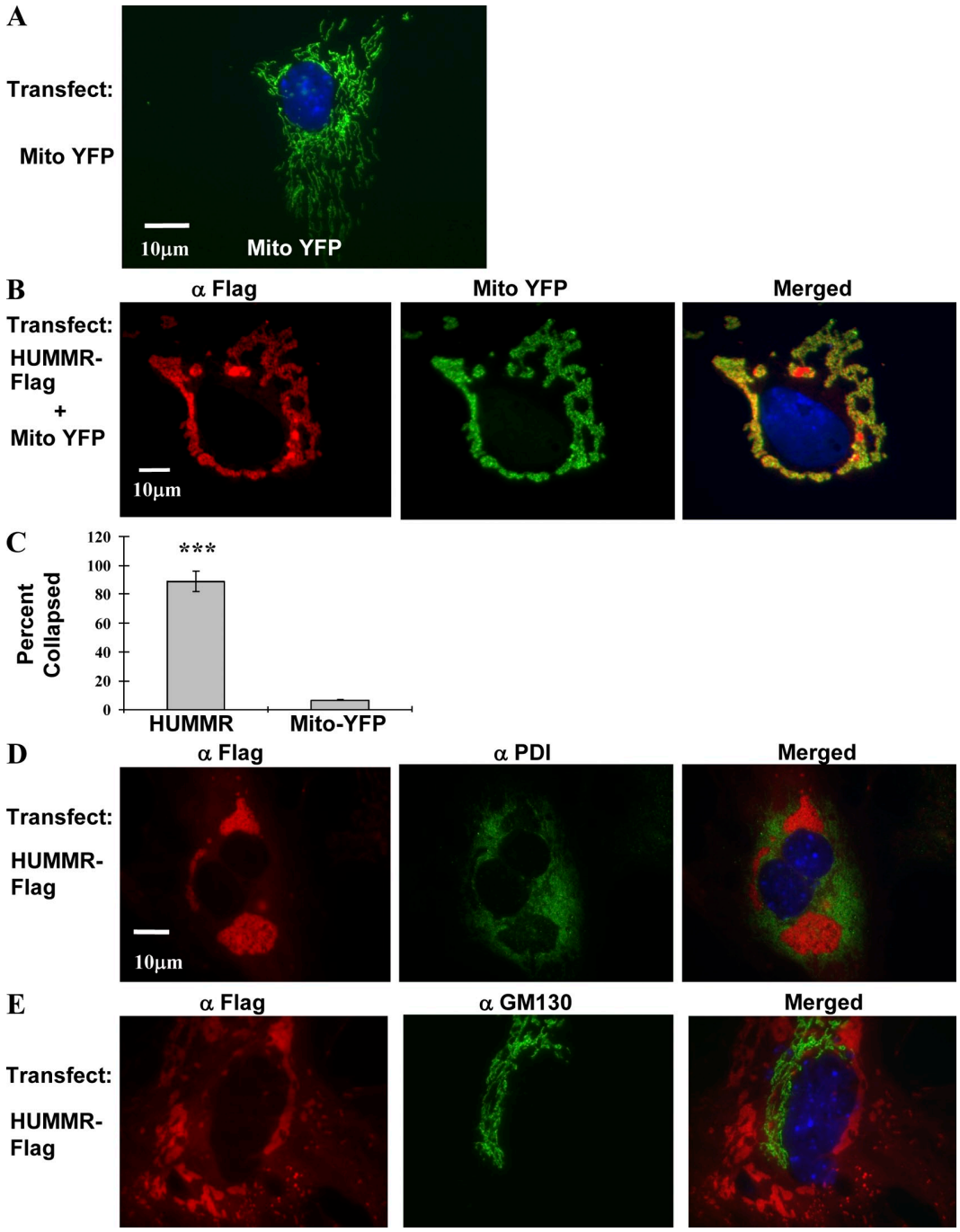

Figure 3. **HUMMR induces collapse of the mitochondrial network.** (A) When transfected alone, mitoYFP labels mitochondria in a diffuse tubular pattern in astrocytes. (B) In contrast, cotransfection of HUMMR-Flag and mitoYFP induces collapse of the mitochondrial network. ICC confirmed that the HUMMR-Flag constructs do not localize to ER (D) or Golgi (E). (C) Quantification of mitochondrial morphology in HUMMR-transfected cells confirms that the majority contain collapsed mitochondrial networks. The scale bar in B, left, applies to all images in B; the scale bar in D applies to all images in D and E. Error bars represent standard deviation averaging three different data points from one representative experiment. (***, $P < 0.001$). All data were replicated in three independent experiments.

Myc–Miro-2 colocalized with HUMMR-V5 (Fig. S4). Similar to the Miros, OIP106 primarily localized to mitochondria when transfected alone and colocalized with HUMMR with cotransfection (Fig. 5, A and B). Yet, unlike the Miros, GRIF-1 and OIP106 are not anchored to the OMM by TMDs, which may increase the probability of a cytoplasmic localization under some conditions. In fact, in only 14 ± 2% of transfected astrocytes was GRIF-1-Flag localized principally to mitochondria (Fig. 5 C). A similar phenomenon was also found to occur in HEK-293 cells (Brickley et al., 2005). In contrast, in the presence of HUMMR-V5, GRIF-1-Flag colocalized with HUMMR-V5 in the collapsed mitochondria in 77 ± 3% of cells (Fig. 5 D). This observation suggests that HUMMR augments the percentage of GRIF-1 localized to the mitochondrial membrane.

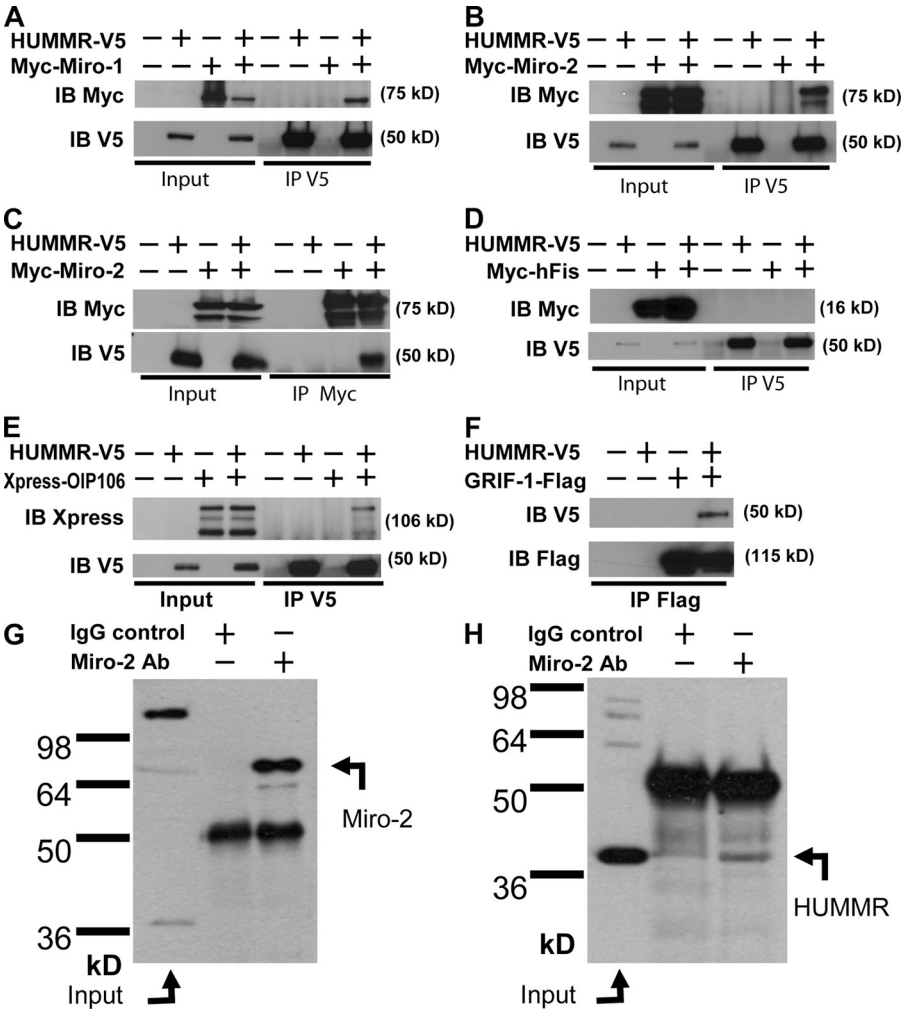

Figure 4. **HUMMR interacts with Miro-1, Miro-2, GRIF-1, and OIP106, but not with hFis-1.** (A and B) HUMMR-V5 was cotransfected into HEK-293 cells with various Miro, GRIF-1, OIP106, or hFis-1 constructs. Using a V5 antibody to IP HUMMR-V5 (IP V5) transfected into HEK-293 cells, Myc–Miro-1 and Myc–Miro-2 bands were identified on an immunoblot (IB Myc). (C) Similarly, Myc antibodies IP a complex containing Myc–Miro-2 and HUMMR-V5. (D) In contrast to Miro-1/Miro-2, no interaction was observed when cotransfecting HUMMR and hFis. (E and F) Similar to the Miro data, using the V5 antibody to IP HUMMR-V5 confirmed that Xpress-OIP106 (E) as well as GRIF-1-Flag (F) were also part of the protein complex. (G and H) An antibody directed against endogenous human Miro-2 effectively IPs Miro-2 (G) and demonstrates a specific interaction with endogenous HUMMR (H), compared with IgG control antibody. All data were replicated in at least three independent experiments.

The C terminus of HUMMR protrudes into the mitochondrial intermembrane space (IMS)

Bas cells are a transformed astrocyte-like cell line with temperature-sensitive large T antigen expression (Bongarzone et al., 1996). Bas cells express HUMMR abundantly under normoxic conditions and were used to explore the submitochondrial localization of HUMMR. Because HUMMR has a TMD and interacts with Miro-1 and Miro-2, it is likely to have one of three topologies (Fig. 6 A): (1) TMD in the OMM with its C terminus in the cytoplasm, (2) TMD in the OMM with its C terminus in the IMS, or (3) TMD in the inner mitochondrial membrane (IMM) with the C terminus in the IMS and interacting with Miro through an undefined protein. To test if HUMMR is tethered to the OMM with its C terminus in the cytoplasm (Fig. 6 A, 1), we exposed isolated mitochondria to trypsin. Unlike the OMM proteins Tom20 and Bcl-2, HUMMR was not degraded by trypsin (Fig. 6 B), which suggests that the C terminus is not in the cytoplasm. Exposure of mitochondria to hypo-osmolar solutions (osmotic shock) induces swelling and permeability of the OMM. Thus, cotreatment of mitochondria with osmotic shock and trypsin allows trypsin to have access to the IMS and degrades proteins in the IMS. Unlike cytochrome *c*, exposure to osmotic shock alone without trypsin did not alter HUMMR protein abundance (Fig. 6 C). Because osmotic shock alone did not reduce HUMMR, this finding suggests that HUMMR is not free to be released from the IMS, perhaps because its TMD is anchored to either the OMM or IMM. Yet, the combined treatment of osmotic shock and trypsin degraded HUMMR, which strongly suggests that HUMMR's C terminus is in the IMS (Fig. 6 C). Similar to the approach used for Bas cells, the topology of HUMMR was also examined in mitochondria isolated from hypoxic neurons (5% O_2 for 24 h). As in Bas cells, the C terminus of HUMMR was located in the IMS, but HUMMR was not released from the IMS with osmotic shock (Fig. 6 D).

Examining the interaction domains of HUMMR and Miro

An analysis of HUMMR topology predicts that the C terminus of HUMMR is located inside the membrane (Tusnady and Simon, 2001), which suggests that the TMD is in the OMM with the C terminus in the IMS. In contrast, if HUMMR is anchored in the IMM, then its C terminus (beyond the TMD) would likely interact either directly or indirectly with Miro (Fig. 6 A, 3). To examine this concept, multiple C-terminal truncation mutants were constructed of HUMMR (Fig. 7 A). When coexpressed with Miro-1 or Miro-2, all of the C-terminal truncation mutants coprecipitated with the Miros, which indicates that the majority of the C terminus beyond the TMD (177 of 219 amino acids) can be eliminated

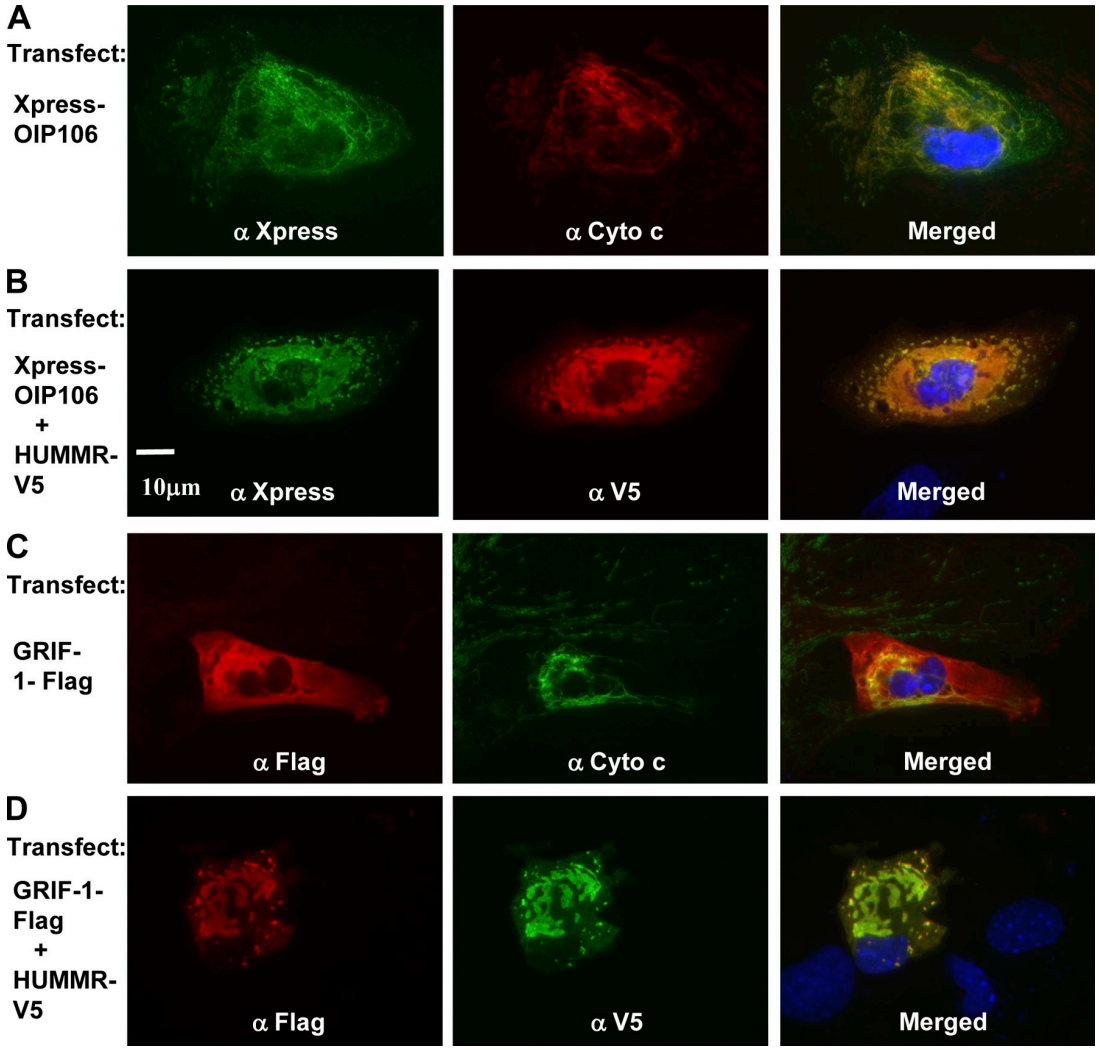

Figure 5. **HUMMR alters localization of GRIF-1.** (A) Transfected Xpress-OIP106 is located primarily in mitochondria. (B) Xpress-OIP106 and HUMMR-V5 colocalize in collapsed mitochondria. (C) Transfected GRIF-1–Flag in astrocytes predominantly localizes to the cytoplasm. (D) Cotransfection of GRIF-1–Flag with HUMMR-V5 demonstrates colocalization of HUMMR-V5 with GRIF-1–Flag to collapsed mitochondria. All data were replicated in three independent experiments.

without interrupting HUMMR–Miro interactions (Fig. 7 B). When larger truncations of the C terminus (>177 aa) were attempted, HUMMR expression was not observed. In contrast to the C terminus, if the N terminus (including TMD) of HUMMR is removed (ΔN1-63-Flag), HUMMR no longer coprecipitates with the Miros. Similarly, when the TMD is removed from Miro-2 (Myc–Miro-2ΔTM), the interaction between HUMMR and Miro-2 is lost (Fig. 7, C and D). However, because ΔN1-63-Flag HUMMR and Myc–Miro-2ΔTM do not traffic to the mitochondria, this is not definitive proof that the proteins are interacting through the N terminus. Yet, these data demonstrate that much of the C terminus of HUMMR is not required for its interaction with the Miros, which suggests that the HUMMR and Miro interact at their TMDs.

Reduced HUMMR function reduces mitochondrial content in axons

To attenuate HUMMR protein abundance and function, small hairpin RNA (shRNA) was designed against HUMMR and expressed with GFP (Fig. S5 A, 1). When delivered by adenovirus to all neurons in culture, the shRNA markedly reduced hypoxia-induced HUMMR protein expression (Fig. S5 B). When neurons are transfected at the time of culture preparation, only 20–30% of neurons are transfected. Despite this small percentage, a reduced abundance of HUMMR is still appreciated in these cultures on day in vitro (DIV) 7 (Fig. S5 C). Similarly, if HUMMR and shRNA are cotransfected into HEK-293 cells, the abundance of transfected HUMMR is diminished in cultures for at least 7 d after transfection (Fig. S5 D).

HUMMR interacts with proteins involved in mitochondrial transport, which are inextricably linked to mitochondrial distribution (Stowers et al., 2002; Guo et al., 2005; Russo et al., 2009). Thus, mitochondrial distribution was examined in the axons of neurons that were cotransfected with shRNA-GFP (or scrambled RNA [scrRNA]-GFP control) and mito-DsRed. Neuronal cultures remained in normoxia from DIV 0–7, or were exposed to 5% oxygen for 24 h on DIV 6, a hypoxia exposure that induces HUMMR expression (Fig. 8 H) without evoking neuronal death. The axons of neurons expressing shRNA (GFP) were identified and the

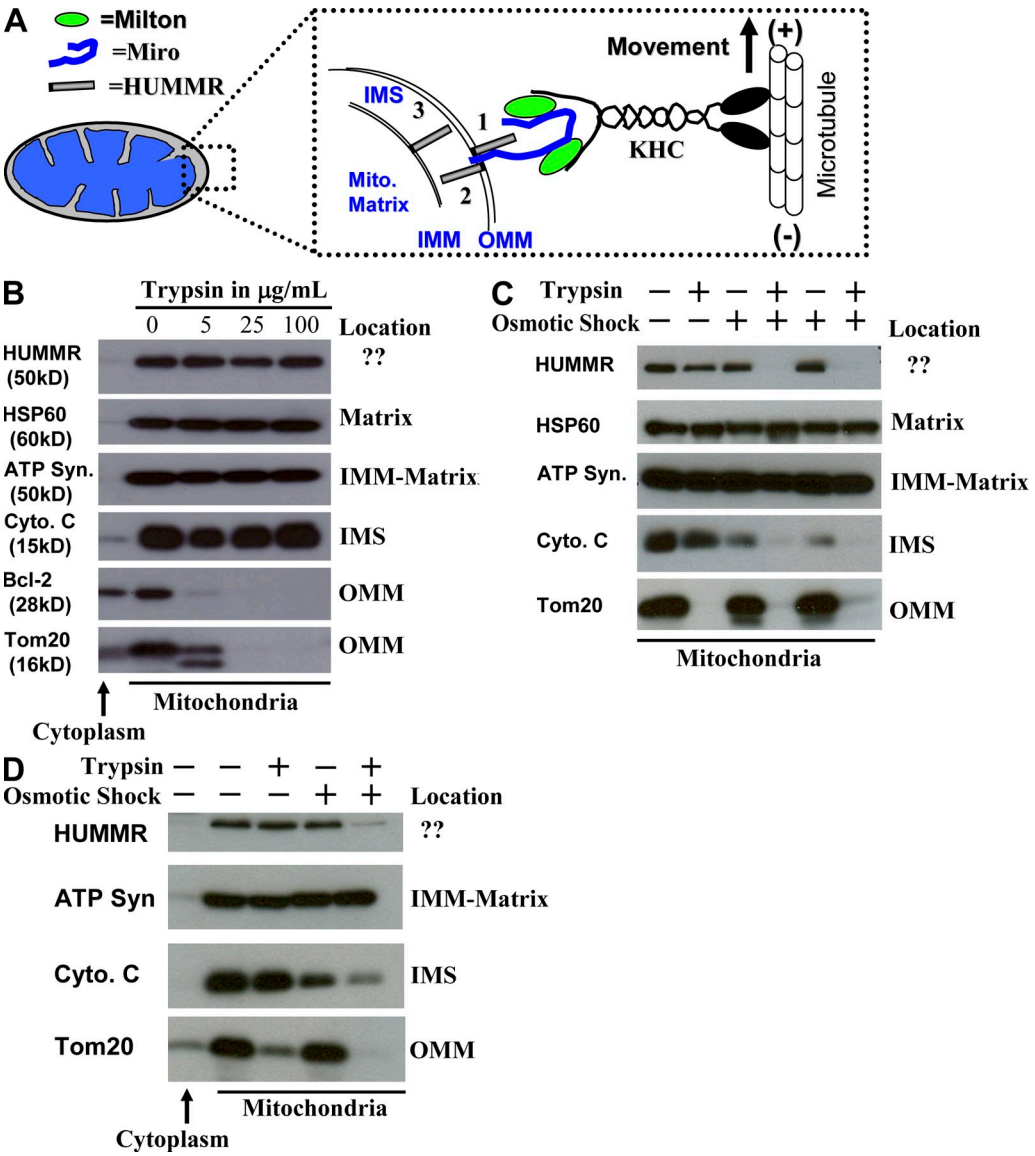

Figure 6. **The C terminus of HUMMR is localized in the IMS.** (A) Because HUMMR interacts with Miro-1 and Miro-2, it likely has one of three conformations: (1) TMD in the OMM with C terminus in cytoplasm, (2) TMD in OMM with C terminus in the IMS, or (3) TMD in the IMM with the C terminus in the IMS. (B) When isolated mitochondria were exposed to trypsin, the OMM proteins Tom20 and Bcl-2 were degraded, but HUMMR was not. (C) To determine if HUMMR's C terminus is in the IMS, mitochondria were subjected to a combination of osmotic shock (which permeabilizes OMM) and trypsin. HUMMR is degraded by combined osmotic shock and trypsin treatment, but not by either treatment alone. As expected, cytochrome *c* was diminished by osmotic shock and then markedly degraded by the combination of osmotic shock and trypsin. (D) When mitochondria are isolated from hypoxic neurons, the same results are observed.

mitochondria contained in the axons were identified (DsRed). The lengths of the mitochondria were measured, summed, and normalized to the length of the axon containing the mitochondria. This measure, termed the mitochondrial axonal index, was a measure of the amount of mitochondria per micrometer of axon, similar to other studies (Saotome et al., 2008; MacAskill et al., 2009a). In normoxia, the mitochondrial axonal index was 0.21 ± 0.007 in scrRNA controls ($n = 3$ independent experiments, 6–8 axons measured per experiment for each treatment group). Hypoxia exposure modestly but significantly increased the mitochondrial axonal index to 0.27 ± 0.007 of the axon ($P < 0.05$, independent *t* test; $n = 3$ experiments). Interestingly, reduced HUMMR function diminished the mitochondrial axonal index by 37 ± 5% in normoxia ($P < 0.01$, independent *t* test; $n = 3$) and by 60 ± 4% ($P < 0.001$, independent *t* test) in hypoxia (Fig. 8 E). This reduction of mitochondrial content in the axon mediated by loss of HUMMR function was greater in hypoxia compared with normoxia ($P < 0.01$, *t* test). The modest induction of mitochondrial axonal index by hypoxia was not observed when HUMMR function was reduced by shRNA (Fig. 8, E and F), which suggests that HUMMR mediates this effect. Similar to mitochondrial axonal index, the number of mitochondria per micrometer of axon was quantified and was reduced by shRNA (Fig. 8 F). Loss of HUMMR function modestly reduced the average individual mitochondrial length (Fig. 8 G).

Because loss of mitochondrial content in the axon would be expected to increase mitochondrial content in the soma, the fluorescence intensity of mito-DsRed was examined in the

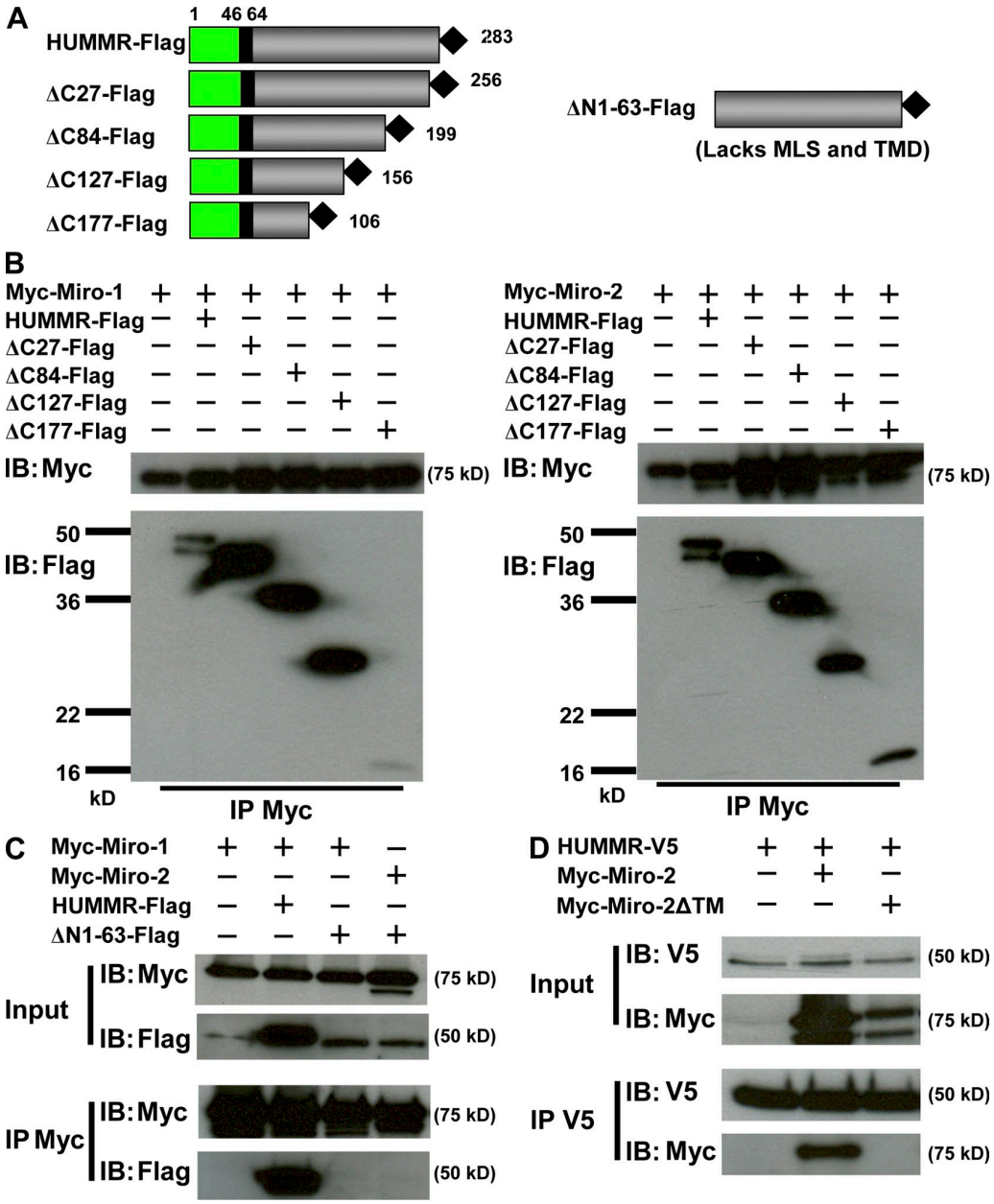

Figure 7. **Loss of the C terminus of HUMMR does not interrupt its binding to Miro.** (A) Schematic diagrams of C terminus and N terminus truncation mutants used for IPs. Numbers indicate amino acids. (B) Truncation of 177 aas of the C terminus of HUMMR does not prevent the interaction of HUMMR with the Miro-1 and Miro-2. (C) Loss of the N terminus of HUMMR interferes with its interaction with Miro-1 and Miro-2. (D) Similarly, loss of the TMD or Miro-2 inhibits its interaction with HUMMR.

neuronal soma. As predicted, reduced HUMMR function enhanced mito-DsRed fluorescence in neuronal soma (Fig. 8 I). In contrast, no change in endo-GFP was observed in the soma, which suggests that the impact of HUMMR is specific for mitochondrial transport and does not alter the distribution of other vesicles (Fig. 8 J).

Loss of HIF-1 function reduces mitochondrial content in axons during hypoxia, which is rescued by HUMMR

Because HUMMR is a HIF-1 target, we reasoned that loss of HIF-1 function would reduce mitochondrial axonal content through loss of HUMMR expression during hypoxia, but would not alter mitochondrial axonal content in normoxia (Fig. 1 D). To examine the effect of loss of HIF-1 function, neurons were prepared from HIF-$1^{F/F}$ (control) or HIF-$1^{F/F}$::EsrCre mice (Fig. 9 A). HIF-$1^{F/F}$::EsrCre mice contain a floxed HIF-1 genomic construct and tamoxifen-activated cre recombinase, allowing for tamoxifen-mediated loss of HIF-1 function in the neurons (Vangeison et al., 2008). As predicted, loss of HIF-1 function reduced the mitochondrial axonal index by 54% ($P < 0.001$, independent *t* test) in neurons exposed to hypoxia, which was not observed in neurons maintained in normoxia (Fig. 9 B). Similarly, mitochondrial number per micrometer of axon was also reduced with loss of HIF-1 function in hypoxia (Fig. 9 C). Because HIF-1 may alter

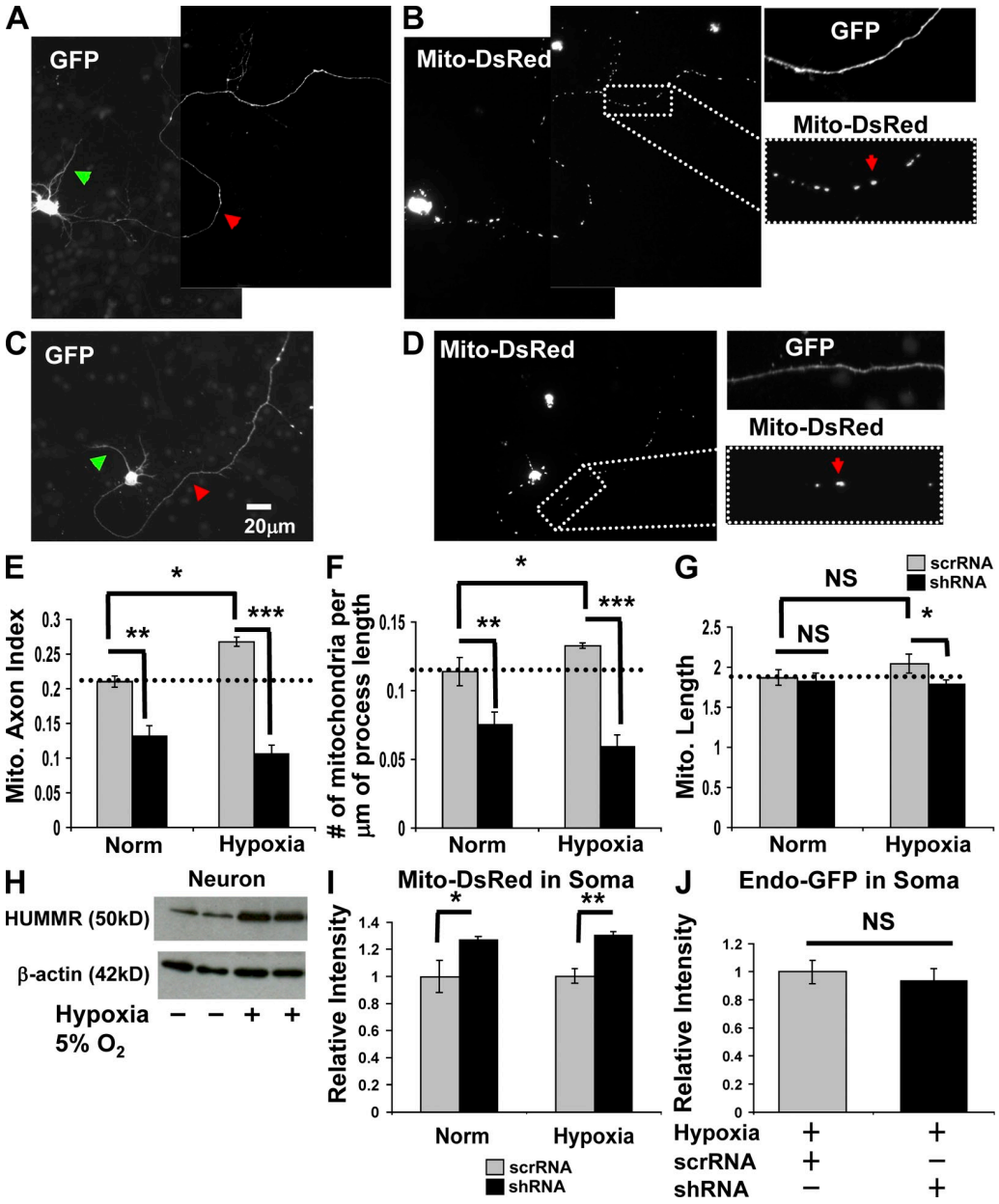

Figure 8. **A reduction in HUMMR function depletes mitochondria in the axon.** (A–D) Cotransfection of shRNA-GFP (A and B) or scrRNA-GFP (C and D); mito-DsRed labels neuronal processes with GFP (A and C; green arrowhead, dendrite; red arrowhead, axon), and mitochondria are labeled with DsRed (B and D). (E and F) Reduced HUMMR function reduces mitochondrial content in the axon (as measured by mitochondrial axonal index; E) and reduces the number of mitochondria per micrometer of axon (F). This effect is more profound in hypoxia. Reduced HUMMR function modestly reduces mean mitochondrial length (G). For ease of comparison, the dotted horizontal lines represent the value of scrRNA controls in normoxia. (H) Exposure of neurons to 5% O_2 for 24 h induces HUMMR protein. (I and J) A reduction in HUMMR function increases mitochondria in the neuronal soma (I) but does not impact Endo-GFP distribution (J). Endo-GFP, GFP tagged endosomes. *, $P < 0.05$; **, $P < 0.01$; ***, $P < 0.001$. Error bars indicate SD; experiments are means of three independent experiments.

mitochondrial biogenesis (Zhang et al., 2007), we examined mitochondrial mass. Loss of HIF-1 function did not reduce mitochondrial mass as judged by the abundance of Tom 20 in neurons exposed to hypoxia for 24 h (Fig. 9 D).

HIF-1 alters mitochondrial oxidative phosphorylation (Kim et al., 2006; Papandreou et al., 2006), which could alter mitochondrial distribution independently of HUMMR. We reasoned that if HIF-1 alters mitochondrial distribution through processes not involving HUMMR, then reducing both HUMMR and HIF-1 function would be expected to reduce mitochondrial axonal content greater than loss of HUMMR function alone. Yet, combined loss of HUMMR and HIF-1 function had no greater effect on the mitochondrial axonal index than loss of HUMMR function alone (Fig. 9 E; $P > 0.05$, independent *t* test). We also explored if HUMMR could rescue the reduced mitochondrial axonal content observed with loss of HIF-1 function. Because high expression levels of HUMMR can induce mitochondrial network collapse (Fig. 3), we cloned mouse HUMMR into a vector (pVax) that displayed lower levels of HUMMR expression. HUMMR successfully rescued axonal mitochondria to baseline

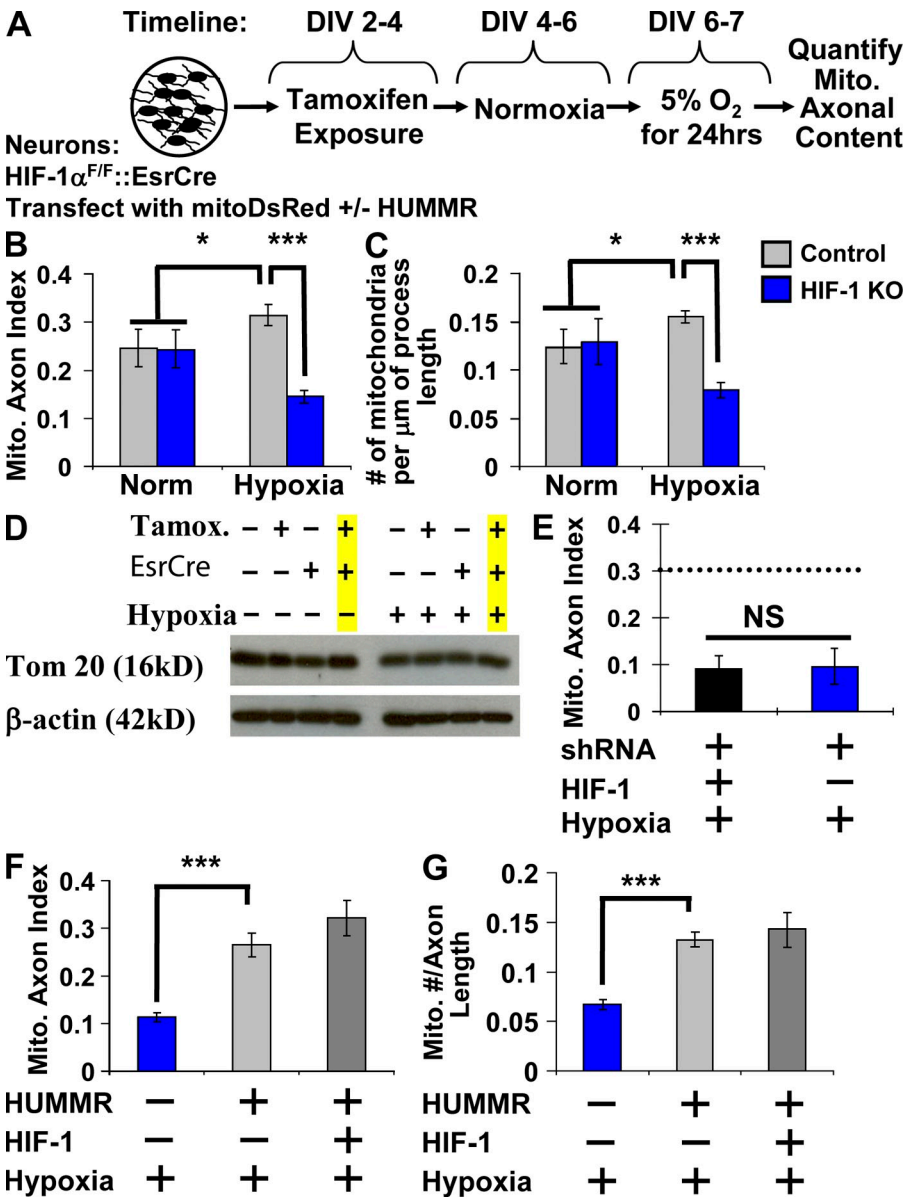

Figure 9. **Loss of HIF-1 function reduces axonal mitochondrial content, which is rescued by HUMMR.** (A) Schematic diagram of an experiment using HIF-1$\alpha^{F/F}$::EsrCre neurons to produce loss of HIF-1 function (± rescue with HUMMR) and its resultant effects on mitochondrial distribution. (B and C) Loss of HIF-1 function reduces axonal mitochondria (as measured by mitochondrial axonal index [B] and mitochondrial number/length of axon [C]) during hypoxia, but is without effect in normoxia (B and C). (D) Loss of HIF-1 function does not alter mitochondrial mass in neurons after 24 h of exposure to 5% O_2. (E) Combined loss of HUMMR and HIF-1 function has no greater effect on the mitochondrial axon index than reduced HUMMR function alone (dotted line indicates baseline level). (F and G) HUMMR rescues the mitochondrial axon content observed with loss of HIF-1 function in hypoxia. NS, nonsignificant. *, $P < 0.05$; ***, $P < 0.001$. Error bars indicate SD; experiments are means of three independent experiments.

levels in hypoxia in HIF-1–null neurons (Fig. 9, F and G). Thus, HUMMR largely mediates HIF-1's influence on mitochondrial distribution in hypoxia.

Reduced HUMMR function diminishes anterograde and increases retrograde mitochondrial transport in hypoxia

Past studies indicate that reduced anterograde transport of mitochondria reduces mitochondria in the axon (Cai et al., 2005). Because HUMMR interacts with the Miros and alters mitochondrial distribution, we examined mitochondrial transport with loss of HUMMR function after transfection of shRNA with coexpression of mito-DsRed (Fig. S5 A, 2). Mitochondrial transport in axons was classified as retrograde or anterograde depending on its direction relative to the cell body, as examined on kymographs (Fig. 10 B).

When examining mitochondrial transport in normoxia or hypoxia, approximately half of motile mitochondria showed anterograde movement (and half retrograde movement) in scrRNA controls ($n = 5$ dishes with 15–25 neurons per data point evaluated; Fig. 10 C). Reducing HUMMR function in normoxia did not significantly alter this balance of directional transport. In contrast, in hypoxia, reduced HUMMR function markedly diminished the percentage of motile mitochondria with anterograde movement, while increasing the percentage transported in the retrograde direction. In hypoxia, 19 ± 9% of motile mitochondria showed anterograde movement in shRNA-transfected cells, whereas 79 ± 6% showed retrograde movement, a highly significant difference ($P < 0.001$, *t* test; $n = 5$; Fig. 10 C). Similarly, loss of HIF-1 function altered mitochondrial transport direction in hypoxia but not normoxia. In hypoxia, 19 ± 4% of motile mitochondria moved in the anterograde direction in HIF-1–null cells, whereas 81 ± 4% moved in the retrograde direction ($P < 0.001$, *t* test; $n = 3$; Fig. 10 D).

In addition to examining the direction of mitochondrial transport, mitochondrial velocity and the percentage of motile

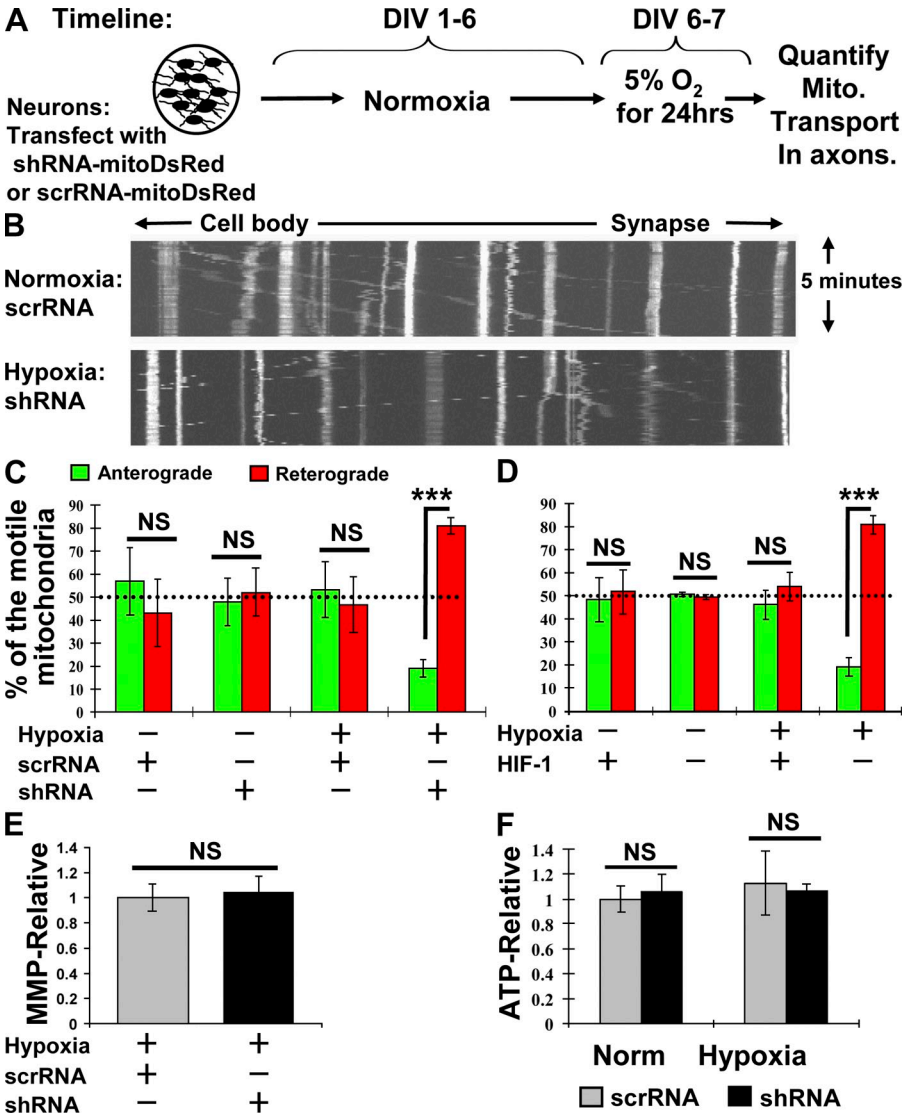

Figure 10. **Reduced HUMMR function diminishes anterograde and enhances retrograde mitochondria.** (A) Schematic diagram of an experiment using shRNA-mito-DsRed to reduce HUMMR function, exposure of neurons to hypoxia, and then the imaging of mitochondrial transport. (B) Examples of kymographs recorded from neurons to determine mitochondrial movement direction. (C and D) Reduced HUMMR function (C) or loss of HIF-1 function (D) reduces the percentage of motile mitochondria that are transported in the anterograde direction and increases the percentage moving in the retrograde direction. Reduced HUMMR function does not alter mitochondrial membrane potential or ATP abundance. The dotted horizontal lines in C and D indicate the point at which an equal number of mitochondria are moving in anterograde and retrograde directions. (E and F) No change in MMP (E) or ATP (F) abundance was observed with reduced HUMMR function. MMP, mitochondrial membrane potential; NS, nonsignificant. ***, $P < 0.001$. Error bars indicate SD; experiments are means of three independent experiments.

mitochondria were quantified. Neither anterograde nor retrograde mitochondrial velocity was diminished by loss of HUMMR or HIF-1 function in normoxia or hypoxia (Table I). In normoxia, the mean velocity of anterograde mitochondria was 0.12 µm/s, which is similar to other studies (Wang and Schwarz, 2009). Anterograde transport velocity was diminished in hypoxia compared with normoxia, but this difference did not reach statistical significance ($P = 0.23$ and $P = 0.08$ for scrRNA and shRNA comparing normoxia and hypoxia, respectively; $n = 5$). In terms of the percentage of mitochondria that are motile, neither shRNA nor loss of HIF-1 function altered the overall percentage of motile mitochondria in normoxia. In normoxia, 15 ± 0.02% and 17 ± 0.04% of mitochondria were motile in the axons of scrRNA- and shRNA-transfected cells, respectively ($P = 0.26$, *t* test; $n = 5$ experiments; $n = 6$ axons in each group per experiment). In normoxia, 15 ± 0.02% and 17 ± 0.04% of mitochondria were motile with wild-type HIF-1 function and with loss of HIF-1 function, respectively ($P > 0.05$, *t* test; $n = 3$ experiments; $n = 6$ axons in each group per experiment). In hypoxia, 11 ± 0.02% and 19 ± 0.03% of mitochondria were motile in the axons of scrRNA- and shRNA-transfected cells, respectively ($P < 0.01$, *t* test; $n = 5$), which was significantly different. Yet, this difference in motility was not observed with loss of HIF-1 function. In hypoxia, 18 ± 0.03% and 20 ± 0.05% of mitochondria were motile in the axons of neurons with and without HIF-1 function, respectively ($P > 0.05$, *t* test; $n = 3$). Because loss of HIF-1 or shRNA function induced similar differences in mitochondrial distribution in hypoxia, and because this phenotype was rescued in HIF-1–null cells by HUMMR (Fig. 9), the significance of this difference in motility seen only with shRNA in hypoxia is uncertain.

In contrast to our finding of 10–20% of mitochondria being motile (see the previous paragraph), past studies suggest that 30–40% of mitochondria are motile (Cai et al., 2005; Chang et al., 2006a; De Vos et al., 2007; Kang et al., 2008). Yet, these studies imaged the cells for 10–15 min or longer. When mitochondrial movement was examined for only 3–4 min (similar to our 5 min), only 12% of the mitochondria were motile (Kuiper et al., 2008). This observation suggests that a greater number of motile mitochondria are captured with longer durations of imaging. In fact, when examined for 15 min, 39 ± 0.05% ($n = 3$ culture dishes; 3–4 cells per dish examined) of mitochondria

Table I. **Mitochondrial velocity**

Condition	Anterograde velocity	Retrograde velocity
	μm/s	*μm/s*
Normoxia: scrRNA	0.12 ± 0.08	0.14 ± 0.06
Normoxia: shRNA	0.11 ± 0.03	0.14 ± 0.04
Hypoxia: scrRNA	0.08 ± 0.02	0.20 ± 0.06
Hypoxia: shRNA	0.07 ± 0.03	0.18 ± 0.06

were motile. This observation suggests that the diminished percentage of motile mitochondria compared with historical controls is related to methodology.

Because mitochondrial membrane potential may impact mitochondrial transport direction (Miller and Sheetz, 2004), we also examined mitochondrial membrane potential. Reduced HUMMR function did not alter mitochondrial membrane potential (Fig. 10 E), which suggests that its impact on mitochondrial transport direction was not due to altered membrane potential. Finally, reduced HUMMR function did not impact ATP abundance (Fig. 10 F).

Discussion

Recent studies link HIF-1 activity with mitochondrial functions including mitochondrial biogenesis, mitochondrial autophagy, electron transport chain function, and reactive oxygen species generation (Kim et al., 2006; Papandreou et al., 2006; Fukuda et al., 2007; Zhang et al., 2007). In this study, we describe another association between HIF-1 and mitochondria, the protein HUMMR (also known as corneal endothelial specific protein). HUMMR is induced by hypoxia through a HIF-1–dependent mechanism and is expressed in neurons, astrocytes, and whole brain. Interestingly, HUMMR interacts with the proteins Miro-1 and Miro-2, and alters localization of GRIF-1, an orthologue of Milton. Loss of HUMMR or HIF-1 function decreased mitochondrial content in axons and reduced anterograde mitochondrial transport. These data strongly suggest that HUMMR is a HIF-1–regulated mitochondrial protein that regulates mitochondrial transport and distribution.

Loss of function of Miro, Milton, or syntabulin, which are all involved in anterograde mitochondrial transport, reduces the mitochondrial number in the axon (Stowers et al., 2002; Cai et al., 2005; Guo et al., 2005; Russo et al., 2009). Similar to these proteins, reduced HUMMR function diminishes the number of mitochondria in the axon. This observation was apparent during normoxia, but was significantly greater after a 24 h exposure to 5% O_2 (Fig. 8 E). When HUMMR function is compromised in hypoxia, anterograde mitochondrial movement is reduced, whereas retrograde mitochondrial transport is enhanced. Although a small trend toward reduced anterograde transport was observed in normoxia, this small change was not significant (Fig. 10 C). This finding, of course, calls into question why reduced HUMMR function would lessen axonal mitochondrial content in normoxia (Fig. 8). The explanation may be due to methodology. It should be appreciated that the HUMMR-targeted shRNA is transfected into neurons at the time the neuronal cultures are prepared, whereas mitochondrial axonal content is not measured until DIV 7. Transfection of shRNA targeting HUMMR in cell lines reduced HUMMR protein for 7 d after transfection. As such, it would be expected that HUMMR function is diminished for multiple days before measuring axonal mitochondrial content on DIV 7. Thus, a small decrease in the probability of anterograde mitochondrial transport may be difficult to appreciate in a few minutes of time-lapsed images. Yet, if present, it may have a large impact on mitochondrial distribution over 7 d. Thus, our methodology for measuring movement may not be sensitive enough to find this modest change in normoxia. We cannot, however, exclude the possibility that HUMMR may have alternative effects on mitochondrial function that diminishes mitochondrial axonal content.

How might HUMMR influence the directional transport of mitochondria? Mitochondria are transported in the axon with periods of transport intermixed with pauses, and may display reversal of direction. As others have suggested (Frederick and Shaw, 2007), this directional movement could be achieved by varying motor recruitment, motor activity, or anchoring of mitochondria. Given that loss of HUMMR or HIF-1 did not alter the mean velocity of mitochondrial transport, a change in motor activity/kinetics is unlikely. Similarly, unlike proteins known to act as anchors for mitochondria (Kang et al., 2008), loss of HUMMR or HIF-1 did not consistently change the percentage of motile mitochondria, although they both reduced the number of mitochondria in the axon, making a change in mitochondrial anchoring unlikely. In contrast, because HUMMR interacts with the Miro–Milton protein complex and induces translocation of GRIF-1 from the cytoplasm to the mitochondria (Fig. 5), it is plausible that HUMMR alters recruitment of GRIF-1 or OIP106 to the OMM, which enhances kinesin motor recruitment. This ability of HUMMR to increase GRIF-1 as part of the protein complex could increase the probability of anterograde movement. Recent work suggests that the GTPase domain of Miro-1 is particularly important for its ability to recruit GRIF-1 to the OMM (MacAskill et al., 2009a). Thus, perhaps HUMMR alters Miro GTPase activity. Yet, a recent study demonstrates that Miro and kinesin heavy chain can directly interact without GRIF-1 (Macaskill et al., 2009b). Moreover, other proteins, including syntabulin and KIF-1–binding protein, alter anterograde transport and localize to the mitochondria (Cai et al., 2005; Wozniak et al., 2005). Putative interactions of HUMMR with these proteins are unexplored.

Given HUMMR's interaction with Miro–Milton, which are directly involved in anterograde transport, it may be surprising that loss of HUMMR function also increased the probability of retrograde transport. It is worth noting that another protein, syntabulin, which influences anterograde movement of mitochondria, does not have this same effect on retrograde movement. When syntabulin function is inhibited, mitochondrial anterograde transport is diminished and the percentage of motile mitochondria declines, but retrograde transport is unchanged (Cai et al., 2005). If loss of HUMMR function diminishes GRIF-1/OIP106 abundance on mitochondria, how would that increase retrograde transport? Perhaps simply reducing the number of anterograde motors attached to a given mitochondria increases the probability of the retrograde motor being engaged, but it is unclear how this would be mediated. Studies suggest that both anterograde and retrograde motors bind simultaneously to bidirectional cargos

and coordinate movement rather than work in opposition (Welte, 2004; Pilling et al., 2006). As such, it is likely that factors that activate anterograde motors also inactivate retrograde motors, and vice versa. Other studies demonstrate an involvement of Miro in anterograde and retrograde transport. For example, when Miro binds calcium, both anterograde and retrograde transport are inhibited (Wang and Schwarz, 2009). Similarly, a recent study demonstrates a fundamental role for Miro in both anterograde and retrograde transport (Russo et al., 2009). The coordination of directional movement is likely complex, as inhibition of the anterograde motor, kinesin 1, inhibits both anterograde and retrograde mitochondrial transport, perhaps suggesting that the kinesins can act as a direct activator of dynein in axons (Pilling et al., 2006). Although $P150^{glued}$, a member of the dynactin protein complex, influences anterograde and retrograde mitochondrial transport, it is unlikely to coordinate directional changes (Pilling et al., 2006). It is still to be determined if HUMMR can interact with or influence the proteins mediating retrograde transport.

Regardless of the mechanism, if HUMMR maintains or enhances mitochondrial transport into axons during hypoxia, this could have important implications for neuronal function. Mitochondrial transport, or lack thereof, modulates synaptic function (Hollenbeck and Saxton, 2005; Chang and Reynolds, 2006; Mattson, 2007). Loss of synaptic mitochondria at neuromuscular synapses in *Drosophila*, induced by loss of dMiro or Dlp1 function, leads to impaired synaptic physiology during prolonged stimulation (Guo et al., 2005; Verstreken et al., 2005). At the neuromuscular junction, loss of mitochondrial-generated ATP leads to diminished recruitment of a reserve pool of synaptic vesicles, which accounts for this loss of synaptic function (Verstreken et al., 2005). Loss of Milton function and mitochondrial transport also impairs synaptic activity of photoreceptors (Stowers et al., 2002). Recent work describes changes in short-term synaptic plasticity with loss of function of syntaphilin, a mitochondrial protein that anchors the mitochondria to axonal microtubules and inhibits transport of mitochondria out of the axon (Kang et al., 2008). In fact, reduced mitochondrial content mediated by loss of syntaphilin function was of a similar magnitude as that induced by loss of HUMMR function. This observation suggests that loss of HUMMR function may similarly alter synaptic plasticity.

Because HUMMR protein abundance is enhanced by hypoxia and HIF-1, its influence on mitochondrial transport/distribution is likely to be most profound with hypoxia/ischemia exposure. It is tempting to speculate that HUMMR function may be particularly important in maintaining or enhancing anterograde mitochondrial transport after focal stroke or global ischemia. This property could maintain/support neuronal and synaptic plasticity, which is prominent in peristroke cortex in the days after ischemia (Carmichael, 2003). Interestingly, synaptic mitochondrial content increases in hippocampal dentate granule cells after transient global ischemia (Briones et al., 2005), which suggests enhanced mitochondrial transport in a condition in which HIF-1 expression is enhanced (Chavez and LaManna, 2002). In support of this idea, we found a modest increase in mitochondrial axonal content after 24 h of hypoxia exposure (Fig. 8), which was abolished when HUMMR function was attenuated. Yet, the impact of hypoxia on mitochondrial transport is only beginning to be explored. A prior study used an acute (6 h) hypoxic (30–40 mm Hg O_2; ~4–6% O_2) insult and observed reduced mitochondrial transport in neuronal processes through a nitric oxide–mediated mechanism (Zanelli et al., 2006). Thus, the responses to hypoxia are likely complex, with diminished mitochondrial movement occuring acutely during hypoxia, which HUMMR expression may counterbalance to improve anterograde transport during longer periods of hypoxia. Beyond its role in hypoxia, HUMMR is present in the brain without exposure of mice to hypoxia (Fig. 1). Moreover, HIF-1 protein abundance, and possibly HUMMR, is increased by stimuli other than hypoxia, such as growth factors (Laughner et al., 2001; Chavez and LaManna, 2002), and in Alzheimer's disease (Soucek et al., 2003). Given that axonal mitochondrial movement is impaired in models of Alzheimer's disease (Ebneth et al., 1998; Pigino et al., 2003; Chang et al., 2006b), enhanced HIF-1 function may help maintain anterograde mitochondrial transport during neurodegeneration.

As described in a previous study, HUMMR is abundant in some tissue, such as testes, ovary, and corneal epithelium in normoxia (Kinouchi et al., 2006). Thus, HUMMR abundance is also regulated by HIF-1–independent mechanisms that are operative under normoxic conditions. The high expression of HUMMR in testes and ovary is of interest because Milton-dependent mitochondrial transport in the oocyte is critical for proper inheritance of mitochondria (Cox and Spradling, 2006). In sperm, loss of Milton function induces deficits in mitochondrial elongation (Aldridge et al., 2007). Thus, HUMMR function may be critical for maintenance of reproductive function and distribution of mitochondria to the embryo.

In summary, we describe the novel finding of a hypoxia and HIF-1–induced mitochondrial protein HUMMR. HUMMR interacts with the mitochondrial transportation molecular machinery, altering the distribution of mitochondria in the axon and modifying the percentage of mitochondria moving in the anterograde direction. These findings may have important consequences for neuronal survival and function.

Materials and methods

Transgenic mice, cell culture, and hypoxic conditions

We used floxed HIF-1α ($HIF\text{-}1\alpha^{F/F}$) mice (a gift of R. Johnson, University of California, San Diego, La Jolla, CA; Ryan et al., 2000), which were crossed with synapsin I cre (Zhu et al., 2001), ESRcre (tamoxifen-inducible B6.Cg-Tg(cre/Esr1); The Jackson Laboratory), and hGFAPcre mice (Zhuo et al., 2001). Primary astrocyte cultures were prepared from postnatal day 0 (P_0) neonatal mice (Rempe et al., 2006). In brief, the brain was removed, then, using a dissecting microscope, the cortex and hippocampus were dissected away from the brain stem. Meninges were removed, and the telencephalon was placed into ice-cold HBSS. The telencephalon was cut into 1-mm cubes and dissociated by repeated pipetting. The cells were pelleted and resuspended with glia minimal essential medium (minimal essential medium [11095–080; Invitrogen] supplemented with 6 g/liter glucose, 1 mM sodium pyruvate, 6% horse serum, and 4% fetal bovine serum). The cells were fed every 3–4 d until they were 100% confluent. Neurons were isolated from embryonic day (E) 14.5 embryos (Rempe et al., 2007). In brief, the embryos were removed and placed into ice-cold Dulbecco's minimal essential medium. Using a dissecting microscope, the cortex and hippocampus were dissected away from the brainstem, the meninges were removed, and the telencephalon was placed into ice-cold HBSS. The tissue was placed in trypsin with EDTA (0.1%) for 20 min, washed three times in Dulbecco's minimal essential medium, and dispersed in neurobasal medium containing B27, L-glutamine, and glutamic acid. The cells were plated in 60-mm plates and maintained in neurobasal media containing B27. HEK-293 cells were

obtained from the American Type Culture Collection and grown in DME with high glucose (Mediatech) supplemented with 10% FCS (Thermo Fisher Scientific), 50 U/ml penicillin, and 50 U/ml streptomycin in a humidified incubator at 37°C under 5% CO_2. Hypoxic exposures were accomplished by placing cultures into a triple gas incubator that replaces oxygen with nitrogen to achieve the desired oxygen percentage (Thermo Fisher Scientific). To attenuate HIF-1 function, neurons were prepared from HIF-1$\alpha^{F/F}$::EsrCre mice and treated with tamoxifen for 48 h, then the tamoxifen was removed by 75% media exchange (Fig. 9 A).

Microarray analysis and quantitative real-time PCR

RNA was isolated from astrocyte or neuronal cultures and treated with DNase according to the manufacturer's instructions (QIAGEN). For microarray analysis, the manufacturer's instructions were followed (CodeLink; GE Healthcare). Synthesis of cDNA used random hexamers as per the manufacture's instructions (SuperScript III; Invitrogen). For quantitative PCR, primer–probe sets were designed with Primer Express III (Applied Biosystems). Primer probe sets for HIF-1α exon 2 were: 5′-TGAACGTCGAAAAGAAAAGTCTAGAG-3′, 5′-GCAAGCTCATAAAAAACTTCAGACTC-3′, and 5′-TGCAGCAAGATCTCGGCGAAGCA-3′ (probe). The primer probes used to detect HUMMR were: 5′-TCCCTGCCGAAGCTGC-3′, 5′-TCGGTTATCTTCAGCTCAGGC-3′, and 5′-TGGTGGAGGCATCCTTATCGAGCTCA-3′ (probe). Transcript was quantified with a sequence detector real-time PCR thermocycler (prism 7300; Applied Biosystems). β-actin served as an internal control.

cDNA and shRNA constructs

Full-length HUMMR cDNA was made by PCR with 5′ primers containing a NotI site and 3′ primers with a Flag or V5 tag followed by HindIII site, and were cloned into pshuttle-cytomegalovirus vector (He et al., 1998). HUMMR ΔC27, ΔC84, ΔC127, ΔC177, and ΔN1-63 with a Flag tag at the C terminal were made by PCR and cloned into a pshuttle-CMV vector. HUMMR-Flag was also cloned into pVAX vector for some experiments. To construct the shRNA-expressing vector, the target sequence and scrambled control were designed using the BIOPREDsi program (www.biopredsi.org) and synthesized by a commercial supplier (Integrated DNA technologies). They were then annealed and cloned into the psuper.neo.GFP vector, which drives expression of the shRNA from an H1 promoter. The H1 and shRNA/scrambled sequences were then subcloned into the pAdTrack (for packaging adenovirus) or mito-DsRed vector (Clontech Laboratories, Inc.) for live cell imaging. Endo-GFP was obtained from Clontech Laboratories, Inc. The following constructs and cells were kindly provided by the investigators as indicated: mito-YFP (provided by R. Tsien, University of California San Diego); rat Flag-tagged GRIF-1 (F.A. Stephenson; School of Pharmacy, University of London, England, UK); human Xpress-OIP106 (G. Hart; Johns Hopkins University School of Medicine, Baltimore, MA); Myc–Miro-1, Myc–Miro-2, and Myc–Miro-2ΔTM (Fransson et al., 2003); Myc-hFis and DRP-1 (Y. Yoon; University of Rochester, Rochester, NY); and Mfn-1 and Mfn-2 double knockout mouse embryonic fibroblasts (D. Chan; California Institute of Technology, Pasadena, CA).

Immunostaining

For ICC, cells were fixed in freshly prepared 4% paraformaldehyde. The cells were permeabilized in blotto (0.9% NaCl, 20 mM Tris buffer, pH 7.5, and 4.5% nonfat dry milk) containing 0.1% Triton X-100 (Sigma-Aldrich), then incubated in primary antibody. Immunostaining was visualized by incubation with appropriate secondary antibodies at 1:1,000 dilutions. The coverslips were mounted on microscope slides with FluorSave reagent (EMD), and cells were visualized with a uPlanFl 40×/0.75 NA or 60×/1.25 NA oil objective lens on a BX61 microscope (all from Olympus). Images were taken with photometrics CoolSNAP camera (Roper Scientific) using IP laboratory software (QImaging). Fluorochromes used were Alexa Fluor 488 and Alexa Fluor 594. Photoshop (Adobe) was used for imaging processing using only linear adjustments of levels or contrast.

For Western blotting, protein lysates were fractionated on 7–12% polyacrylamide-SDS gel and transferred to polyvinylidene fluoride membranes (Bio-Rad Laboratories). Membranes were blocked in blocking buffer (PBS containing 4% nonfat dry milk) for 1 h at room temperature. Membranes were transferred to a primary antibody dilution and incubated overnight at 4°C. After washed three times with PBS, membranes were incubated with HRP-conjugated secondary antibody diluted for 1 h at room temperature, washed with PBS, and then exposed to chemiluminescence substrate (Western Lightening; PerkinElmer).

Anti–mouse HUMMR polyclonal antibody was produced by immunizing two rabbits with synthetic peptide corresponding to residues Ser^{259}-Gly^{283} of mouse HUMMR, then the sera was pooled and the antibody isolated (Thermo Fisher Scientific). Anti–human HUMMR antibody was produced by immunizing rabbits with synthetic peptide corresponding to residues (Glu^{216}-Gly^{240}) of human HUMMR (Thermo Fisher Scientific). Antibody was purified from immune serum by affinity chromatography. Anti–human Miro-2 polyclonal antibody was produced by immunizing rabbits with a synthetic peptide corresponding to amino acid residues Cys79–Ile93 of human Miro-2 (Agrisera). Other antibodies used include: mouse and rabbit anti-Flag (M2; Sigma-Aldrich), mouse anti-V5 (Invitrogen), rabbit anti-V5 (Immunology Consultants Laboratory, Inc.), mouse anti-Myc (Cell Signaling Technology), rabbit anti-Myc (Abcam), mouse anti–cytochrome *c* (BD), mouse anti–α-tubulin (Sigma-Aldrich), mouse anti-GM130 (Abcam), and mouse anti–protein disulfide isomerase (Abcam). Filamentous actin was visualized by TRITC-conjugated phalloidin (Sigma-Aldrich). The following fluorescently labeled secondary antibodies were used: goat anti–mouse Alexa Fluor 488, goat anti–mouse Alexa Fluor 594, goat anti–rabbit Alexa Fluor 488, and goat anti–rabbit Alexa Fluor 594 (Invitrogen).

IPs

To perform IPs, HEK-293 cells were cotransfected with the relevant constructs. 48 h after transfection, cells were collected in PBS and lysed in lysis buffer (10 mM Tris buffer, pH 8.0, 5 mM EDTA, 150 mM NaCl, 1 mM iodoacetamide, and 1% Triton X-100) containing 1 mM PMSF and protease inhibitor (Sigma-Aldrich). Primary antibodies were added to cell lysate and incubated at 4°C overnight. Protein A–agarose (Santa Cruz Biotechnology, Inc.) was used to elute the antibody protein complex. For IP of endogenous Miro-2 and hHUMMR, human Miro-2 antibody was used to immunoprecipitate Miro-2. The eluted IP complex was tested against hHUMMR to test the endogenous interaction.

Mitochondria isolation from cells

Cells were collected in cold isolation buffer (320 mM sucrose, 10 mM Hepes, and 1 mM EDTA, pH 7.2) and lysed in N2 cavitation bomb under 2,000 psi. Homogenates were centrifuged at 700 *g* for 8 min, the supernatant was collected, and the pellet was resuspended and recentrifuged at 700 *g* for 3 min. The combined first and second supernatant was centrifuged at 8,000 *g* for 11 min to pellet the mitochondria. Mitochondria pellet was washed three times and resuspended in 50 µl of buffer for further analysis.

For osmotic shock, 10 µl of the mitochondria preparation was mixed with 490 µl of 10 mM potassium phosphate buffer, pH 7.2, and left on ice for 20 min. The content of the tube was then pipetted 10 times to facilitate permeabilization of the OMM. Mitochondria were centrifuged in a cold room at 8,000 *g* for 11 min and resuspended in isolation buffer for the trypsin treatment (0, 5, 25, or 100 µg/ml trypsin for 30 min at room temperature). At the end of digestion, trypsin was removed by centrifugation and the mitochondria pellet was washed before Western blot analysis.

Measuring anterograde and retrograde mitochondrial transport

When examining the impact of HUMMR on mitochondrial transport, E14 mouse cortical neurons were transfected with mito-DsRed-H1-shRNA– or mito-DsRed-H1-scrRNA–expressing vectors at the time of neuronal culture preparation and before plating (Halterman et al., 2009). When examining the impact of loss of HIF-1 function on mitochondrial transport, neuronal cultures were prepared from E14 HIF-1$^{F/F}$::EsrCre (test) or HIF-1$^{F/F}$ (control) mouse cortical neurons. These neurons were transfected with mito-DsRed at the time of preparation (Halterman et al., 2009). These cultures were subsequently exposed to 100 nM tamoxifen to eliminate HIF-1 function (Vangeison et al., 2008). On DIV 7, imaging of DsRed (+) mitochondria allowed for identification of transfected neurons (Fig. 8 B). Imaging of mitochondrial movement was performed similar to others (Ligon and Steward, 2000a,b; Zanelli et al., 2006). The samples were maintained at 37°C (in 5% CO_2 to maintain pH) in phenol red–free neurobasal medium supplemented with 10 mM Hepes, while mitochondrial images (RETIGA EXi cooled camera driven by IP laboratory software) were obtained on an inverted microscope (IX70; Olympus) with an Ach 60×/0.80 NA objective lens (Olympus) every 5 s for 5 min using 75 ms (VMM-D1 shutter drive; Uniblitz) of light exposure (mercury light source) per image. The light source was attenuated by 90% with neutral density filters to prevent phototoxicity. We selected axonal processes for quantitative analysis of mitochondrial movement. Axonal processes were chosen for recordings based on known morphological characteristics (Banker and Cowan, 1979). A neuronal process was considered an axon if it was at least twice the length of any of the other processes and did not taper during its course. Only those that appeared to be single axons and isolated from other transfected neurons in the field were chosen. Mitochondrial movement was imaged in 3–5 different dishes (3–5 axons per dish and 60–80 mitochondria per dish) of neurons for each condition. Thus, when combining three independent experiments, a total of ∼15 axons and 180–300 mitochondria

were measured in each condition. MetaMorph 6.1 software (MDS Analytical Technologies) was used to generate a kymograph for each field. A movement was counted only if the net displacement was at least 2.5 µm within the 5-min time frame. The net direction of movement was determined by comparing the net displacement between its initial and final positions relative to the cell body.

Quantifying mitochondria content in axons and cell body

E14 C57 mouse embryos were used to prepare neuronal cultures. Neurons were cotransfected by psuper.GFP-shRNA (or GFP-scrRNA) and mito-DsRed vectors at DIV 0. In some cases, endo-GFP (Clontech Laboratories, Inc.) was transfected in the neurons. The cultures were maintained in normoxia until DIV 6, exposed to 5% O_2 for 24 h from DIV 6–7, and then fixed in 4% paraformaldehyde. ICC was performed with a GFP antibody (Invitrogen). For imaging, the axons of single neurons were traced, and GFP and mito-DsRed images were obtained for each field and colocalized. In general, the axon of each neuron was traced for up to 500 µm, the number of mitochondria in the axon was counted, and their lengths were measured by MetaMorph software. Mitochondrial lengths were summed and divided by the axon length to get the mitochondrial axonal index (average mitochondrial length per micrometer of axon; Saotome et al., 2008; MacAskill et al., 2009a). We also measured mean fluorescence intensity of mito-DsRed in cell bodies expressing either shRNA or scrRNA as an indication of mitochondrial abundance in cell bodies.

ATP and mitochondria membrane potential measurement

E14 C57 mouse cortical neurons were plated and infected by lentivirus-expressing shRNA or scrRNA on DIV 2; 100% infection efficiency was achieved and confirmed by looking at GFP^+ cells. Cells were kept in normoxia until DIV 6 and exposed to 5% oxygen for 24 h from DIV 6–7. At DIV 7, cellular ATP level was measured using an ATP bioluminescent assay kit (Sigma-Aldrich) according to the manufacturer's instructions. In separate cultures, 5 nM tetramethyl rhodamine methyl ester was used to measure mitochondrial membrane potential by comparing fluorescence intensity between groups.

Online supplemental material

Fig. S1 shows images of the intracellular cytoskeleton with HUMMR expression. Fig. S2 illustrates that loss of mitochondrial fusion or enhanced mitochondrial fission does not alter HUMMR-induced mitochondrial network collapse. Fig. S3 demonstrates the characterization of human Miro-2 and hHUMMR antibody. Fig. S4 shows colocalization of Miro-1 and Miro-2 with HUMMR by ICC. Fig. S5 demonstrates the effectiveness of shRNA in knocking down HUMMR. Table S1 lists multiple transcripts found on microarray to be regulated by HIF-1. Online supplemental material is available at http://www.jcb.org/cgi/content/full/jcb.200811033/DC1.

We thank several investigators for providing reagents for these studies, including Dr. Randall Johnson, Dr. F. Anne Stephenson, Dr. Gerald Hart, Dr. Roger Tsien, and Dr. David Chan. We appreciated advice of Dr. Paul Brookes regarding experiments requiring mitochondrial isolation and trypsin/osmotic shock. We thank Dr. Pat Trimmer and Dr. Nina Solenski for expertise with mitochondrial transport methodology. We would also like to thank Dr. Handy Gelbard, Dr. Seth Perry, Dr. Yisang Yoon, and Dr. Tom Schwarz for critically reading earlier versions of the manuscript. We thank Maria Jepson, Landa Prifti, and Rita Giuliano for excellent technical assistance.

This research was supported in part by a K08 award (NS046633 to D.A. Rempe) and a grant (1P01NS050315) from the National Institute of Neurological Disorders and Stroke.

Submitted: 7 November 2008
Accepted: 14 May 2009

References

Aldridge, A.C., L.P. Benson, M.M. Siegenthaler, B.T. Whigham, R.S. Stowers, and K.G. Hales. 2007. Roles for Drp1, a dynamin-related protein, and milton, a kinesin-associated protein, in mitochondrial segregation, unfurling and elongation during *Drosophila* spermatogenesis. *Fly (Austin).* 1:38–46.

Banker, G.A., and W.M. Cowan. 1979. Further observations on hippocampal neurons in dispersed cell culture. *J. Comp. Neurol.* 187:469–493.

Bongarzone, E.R., L.M. Foster, S. Byravan, A.N. Verity, C.F. Landry, V.V. Schonmann, S. Amur-Umarjee, and A.T. Campagnoni. 1996. Conditionally immortalized neural cell lines: potential models for the study of neural cell function. *Methods.* 10:489–500.

Brickley, K., M.J. Smith, M. Beck, and F.A. Stephenson. 2005. GRIF-1 and OIP106, members of a novel gene family of coiled-coil domain proteins: association in vivo and in vitro with kinesin. *J. Biol. Chem.* 280:14723–14732.

Briones, T.L., E. Suh, L. Jozsa, M. Rogozinska, J. Woods, and M. Wadowska. 2005. Changes in number of synapses and mitochondria in presynaptic terminals in the dentate gyrus following cerebral ischemia and rehabilitation training. *Brain Res.* 1033:51–57.

Cai, Q., C. Gerwin, and Z.H. Sheng. 2005. Syntabulin-mediated anterograde transport of mitochondria along neuronal processes. *J. Cell Biol.* 170:959–969.

Carmichael, S.T. 2003. Plasticity of cortical projections after stroke. *Neuroscientist.* 9:64–75.

Chang, D.T., and I.J. Reynolds. 2006. Mitochondrial trafficking and morphology in healthy and injured neurons. *Prog. Neurobiol.* 80:241–268.

Chang, D.T., A.S. Honick, and I.J. Reynolds. 2006a. Mitochondrial trafficking to synapses in cultured primary cortical neurons. *J. Neurosci.* 26:7035–7045.

Chang, D.T., G.L. Rintoul, S. Pandipati, and I.J. Reynolds. 2006b. Mutant huntingtin aggregates impair mitochondrial movement and trafficking in cortical neurons. *Neurobiol. Dis.* 22:388–400.

Chavez, J.C., and J.C. LaManna. 2002. Activation of hypoxia-inducible factor-1 in the rat cerebral cortex after transient global ischemia: potential role of insulin-like growth factor-1. *J. Neurosci.* 22:8922–8931.

Chen, H., S.A. Detmer, A.J. Ewald, E.E. Griffin, S.E. Fraser, and D.C. Chan. 2003. Mitofusins Mfn1 and Mfn2 coordinately regulate mitochondrial fusion and are essential for embryonic development. *J. Cell Biol.* 160:189–200.

Claros, M.G., and P. Vincens. 1996. Computational method to predict mitochondrially imported proteins and their targeting sequences. *Eur. J. Biochem.* 241:779–786.

Cox, R.T., and A.C. Spradling. 2006. Milton controls the early acquisition of mitochondria by *Drosophila* oocytes. *Development.* 133:3371–3377.

De Vos, K.J., A.L. Chapman, M.E. Tennant, C. Manser, E.L. Tudor, K.F. Lau, J. Brownlees, S. Ackerley, P.J. Shaw, D.M. McLoughlin, et al. 2007. Familial amyotrophic lateral sclerosis-linked SOD1 mutants perturb fast axonal transport to reduce axonal mitochondria content. *Hum. Mol. Genet.* 16:2720–2728.

Ebneth, A., R. Godemann, K. Stamer, S. Illenberger, B. Trinczek, and E. Mandelkow. 1998. Overexpression of tau protein inhibits kinesin-dependent trafficking of vesicles, mitochondria, and endoplasmic reticulum: implications for Alzheimer's disease. *J. Cell Biol.* 143:777–794.

Fransson, A., A. Ruusala, and P. Aspenstrom. 2003. Atypical Rho GTPases have roles in mitochondrial homeostasis and apoptosis. *J. Biol. Chem.* 278:6495–6502.

Fransson, S., A. Ruusala, and P. Aspenstrom. 2006. The atypical Rho GTPases Miro-1 and Miro-2 have essential roles in mitochondrial trafficking. *Biochem. Biophys. Res. Commun.* 344:500–510.

Frederick, R.L., and J.M. Shaw. 2007. Moving mitochondria: establishing distribution of an essential organelle. *Traffic.* 8:1668–1675.

Frederick, R.L., J.M. McCaffery, K.W. Cunningham, K. Okamoto, and J.M. Shaw. 2004. Yeast Miro GTPase, Gem1p, regulates mitochondrial morphology via a novel pathway. *J. Cell Biol.* 167:87–98.

Fukuda, R., H. Zhang, J.W. Kim, L. Shimoda, C.V. Dang, and G.L. Semenza. 2007. HIF-1 regulates cytochrome oxidase subunits to optimize efficiency of respiration in hypoxic cells. *Cell.* 129:111–122.

Glater, E.E., L.J. Megeath, R.S. Stowers, and T.L. Schwarz. 2006. Axonal transport of mitochondria requires milton to recruit kinesin heavy chain and is light chain independent. *J. Cell Biol.* 173:545–557.

Gorska-Andrzejak, J., R.S. Stowers, J. Borycz, R. Kostyleva, T.L. Schwarz, and I.A. Meinertzhagen. 2003. Mitochondria are redistributed in *Drosophila* photoreceptors lacking milton, a kinesin-associated protein. *J. Comp. Neurol.* 463:372–388.

Guo, X., G.T. Macleod, A. Wellington, F. Hu, S. Panchumarthi, M. Schoenfield, L. Marin, M.P. Charlton, H.L. Atwood, and K.E. Zinsmaier. 2005. The GTPase dMiro is required for axonal transport of mitochondria to *Drosophila* synapses. *Neuron.* 47:379–393.

Halterman, M.W., R. Giuliano, C. Dejesus, and N.F. Schor. 2009. In-tube transfection improves the efficiency of gene transfer in primary neuronal cultures. *J. Neurosci. Methods.* 177:348–354.

He, T.C., S. Zhou, L.T. da Costa, J. Yu, K.W. Kinzler, and B. Vogelstein. 1998. A simplified system for generating recombinant adenoviruses. *Proc. Natl. Acad. Sci. USA.* 95:2509–2514.

Hollenbeck, P.J., and W.M. Saxton. 2005. The axonal transport of mitochondria. *J. Cell Sci.* 118:5411–5419.

Kang, J.S., J.H. Tian, P.Y. Pan, P. Zald, C. Li, C. Deng, and Z.H. Sheng. 2008. Docking of axonal mitochondria by syntaphilin controls their mobility and affects short-term facilitation. *Cell.* 132:137–148.

Kietzmann, T., W. Knabe, and R. Schmidt-Kastner. 2001. Hypoxia and hypoxia-inducible factor modulated gene expression in brain: involvement in

neuroprotection and cell death. *Eur. Arch. Psychiatry Clin. Neurosci.* 251:170–178.

Kim, J.W., I. Tchernyshyov, G.L. Semenza, and C.V. Dang. 2006. HIF-1-mediated expression of pyruvate dehydrogenase kinase: a metabolic switch required for cellular adaptation to hypoxia. *Cell Metab.* 3:177–185.

Kinouchi, R., T. Kinouchi, T. Hamamoto, T. Saito, A. Tavares, T. Tsuru, and S. Yamagami. 2006. Distribution of CESP-1 protein in the corneal endothelium and other tissues. *Invest. Ophthalmol. Vis. Sci.* 47:1397–1403.

Kuiper, J.W., F.T. Oerlemans, J.A. Fransen, and B. Wieringa. 2008. Creatine kinase B deficient neurons exhibit an increased fraction of motile mitochondria. *BMC Neurosci.* 9:73.

Laughner, E., P. Taghavi, K. Chiles, P.C. Mahon, and G.L. Semenza. 2001. HER2 (neu) signaling increases the rate of hypoxia-inducible factor 1alpha (HIF-1alpha) synthesis: novel mechanism for HIF-1-mediated vascular endothelial growth factor expression. *Mol. Cell. Biol.* 21:3995–4004.

Ligon, L.A., and O. Steward. 2000a. Movement of mitochondria in the axons and dendrites of cultured hippocampal neurons. *J. Comp. Neurol.* 427:340–350.

Ligon, L.A., and O. Steward. 2000b. Role of microtubules and actin filaments in the movement of mitochondria in the axons and dendrites of cultured hippocampal neurons. *J. Comp. Neurol.* 427:351–361.

Llopis, J., J.M. McCaffery, A. Miyawaki, M.G. Farquhar, and R.Y. Tsien. 1998. Measurement of cytosolic, mitochondrial, and Golgi pH in single living cells with green fluorescent proteins. *Proc. Natl. Acad. Sci. USA.* 95:6803–6808.

Ly, C.V., and P. Verstreken. 2006. Mitochondria at the synapse. *Neuroscientist.* 12:291–299.

MacAskill, A.F., K. Brickley, F.A. Stephenson, and J.T. Kittler. 2009a. GTPase dependent recruitment of Grif-1 by Miro1 regulates mitochondrial trafficking in hippocampal neurons. *Mol. Cell. Neurosci.* 40:301–312.

Macaskill, A.F., J.E. Rinholm, A.E. Twelvetrees, I.L. Arancibia-Carcamo, J. Muir, A. Fransson, P. Aspenstrom, D. Attwell, and J.T. Kittler. 2009b. Miro1 is a calcium sensor for glutamate receptor-dependent localization of mitochondria at synapses. *Neuron.* 61:541–555.

Mattson, M.P. 2007. Mitochondrial regulation of neuronal plasticity. *Neurochem. Res.* 32:707–715.

Miller, K.E., and M.P. Sheetz. 2004. Axonal mitochondrial transport and potential are correlated. *J. Cell Sci.* 117:2791–2804.

Papandreou, I., R.A. Cairns, L. Fontana, A.L. Lim, and N.C. Denko. 2006. HIF-1 mediates adaptation to hypoxia by actively downregulating mitochondrial oxygen consumption. *Cell Metab.* 3:187–197.

Pigino, G., G. Morfini, A. Pelsman, M.P. Mattson, S.T. Brady, and J. Busciglio. 2003. Alzheimer's presenilin 1 mutations impair kinesin-based axonal transport. *J. Neurosci.* 23:4499–4508.

Pilling, A.D., D. Horiuchi, C.M. Lively, and W.M. Saxton. 2006. Kinesin-1 and dynein are the primary motors for fast transport of mitochondria in *Drosophila* motor axons. *Mol. Biol. Cell.* 17:2057–2068.

Rempe, D., G. Vangeison, J. Hamilton, Y. Li, M. Jepson, and H.J. Federoff. 2006. Synapsin I Cre transgene expression in male mice produces germline recombination in progeny. *Genesis.* 44:44–49.

Rempe, D.A., K.M. Lelli, G. Vangeison, R.S. Johnson, and H.J. Federoff. 2007. In cultured astrocytes, p53 and MDM2 do not alter hypoxia-inducible factor-1{alpha} function regardless of the presence of DNA damage. *J. Biol. Chem.* 282:16187–16201.

Russo, G.J., K. Louie, A. Wellington, G.T. Macleod, F. Hu, S. Panchumarthi, and K.E. Zinsmaier. 2009. *Drosophila* Miro is required for both anterograde and retrograde axonal mitochondrial transport. *J. Neurosci.* 29:5443–5455.

Ryan, H.E., M. Poloni, W. McNulty, D. Elson, M. Gassmann, J.M. Arbeit, and R.S. Johnson. 2000. Hypoxia-inducible factor-1a is a positive factor in solid tumor growth. *Cancer Res.* 60:4010–4015.

Santel, A., S. Frank, B. Gaume, M. Herrler, R.J. Youle, and M.T. Fuller. 2003. Mitofusin-1 protein is a generally expressed mediator of mitochondrial fusion in mammalian cells. *J. Cell Sci.* 116:2763–2774.

Saotome, M., D. Safiulina, G. Szabadkai, S. Das, A. Fransson, P. Aspenstrom, R. Rizzuto, and G. Hajnoczky. 2008. Bidirectional Ca2+-dependent control of mitochondrial dynamics by the Miro GTPase. *Proc. Natl. Acad. Sci. USA.* 105:20728–20733.

Semenza, G.L. 2000a. HIF-1 and human disease: one highly involved factor. *Genes Dev.* 14:1983–1991.

Semenza, G.L. 2000b. HIF-1: mediator of physiological and pathophysiological responses to hypoxia. *J. Appl. Physiol.* 88:1474–1480.

Semenza, G.L. 2008. Mitochondrial autophagy: life and breath of the cell. *Autophagy.* 4:534–536.

Soucek, T., R. Cumming, R. Dargusch, P. Maher, and D. Schubert. 2003. The regulation of glucose metabolism by HIF-1 mediates a neuroprotective response to amyloid beta peptide. *Neuron.* 39:43–56.

Stowers, R.S., L.J. Megeath, J. Gorska-Andrzejak, I.A. Meinertzhagen, and T.L. Schwarz. 2002. Axonal transport of mitochondria to synapses depends on milton, a novel *Drosophila* protein. *Neuron.* 36:1063–1077.

Tusnady, G.E., and I. Simon. 2001. The HMMTOP transmembrane topology prediction server. *Bioinformatics.* 17:849–850.

Vangeison, G., D. Carr, H.J. Federoff, and D.A. Rempe. 2008. The good, the bad, and the cell type-specific roles of hypoxia inducible factor-1alpha in neurons and astrocytes. *J. Neurosci.* 28:1988–1993.

Verstreken, P., C.V. Ly, K.J. Venken, T.W. Koh, Y. Zhou, and H.J. Bellen. 2005. Synaptic mitochondria are critical for mobilization of reserve pool vesicles at *Drosophila* neuromuscular junctions. *Neuron.* 47:365–378.

Wang, X., and T.L. Schwarz. 2009. The mechanism of Ca2+ -dependent regulation of kinesin-mediated mitochondrial motility. *Cell.* 136:163–174.

Welte, M.A. 2004. Bidirectional transport along microtubules. *Curr. Biol.* 14:R525–R537.

Wenger, R.H. 2000. Mammalian oxygen sensing, signalling and gene regulation. *J. Exp. Biol.* 203:1253–1263.

Wozniak, M.J., M. Melzer, C. Dorner, H.U. Haring, and R. Lammers. 2005. The novel protein KBP regulates mitochondria localization by interaction with a kinesin-like protein. *BMC Cell Biol.* 6:35.

Zanelli, S.A., P.A. Trimmer, and N.J. Solenski. 2006. Nitric oxide impairs mitochondrial movement in cortical neurons during hypoxia. *J. Neurochem.* 97:724–736.

Zhang, H., P. Gao, R. Fukuda, G. Kumar, B. Krishnamachary, K.I. Zeller, C.V. Dang, and G.L. Semenza. 2007. HIF-1 inhibits mitochondrial biogenesis and cellular respiration in VHL-deficient renal cell carcinoma by repression of C-MYC activity. *Cancer Cell.* 11:407–420.

Zhang, H., M. Bosch-Marce, L.A. Shimoda, Y.S. Tan, J.H. Baek, J.B. Wesley, F.J. Gonzalez, and G.L. Semenza. 2008. Mitochondrial autophagy is an HIF-1-dependent adaptive metabolic response to hypoxia. *J. Biol. Chem.* 283:10892–10903.

Zhu, Y., M.I. Romero, P. Ghosh, Z. Ye, P. Charnay, E.J. Rushing, J.D. Marth, and L.F. Parada. 2001. Ablation of NF1 function in neurons induces abnormal development of cerebral cortex and reactive gliosis in the brain. *Genes Dev.* 15:859–876.

Zhuo, L., M. Theis, I. Alvarez-Maya, M. Brenner, K. Willecke, and A. Messing. 2001. hGFAP-cre transgenic mice for manipulation of glial and neuronal function in vivo. *Genesis.* 31:85–94.